



Integrated seawater intrusion and groundwater quality assessment of a coastal aquifer: GALDIT, geospatial and analytical approaches

Temitope Ezekiel Idowu^{1,2} · Charlyne Jepkosgei³ · Maurice Nyadawa⁴ · Maurice O. Korowe^{4,5} · Rose M. Waswa⁶ · Kayode H. Lasisi^{7,8} · Nelly Kiplangat¹ · Jane Munyi¹ · Fidelis O. Ajibade⁸

Received: 12 July 2021 / Accepted: 9 December 2021 / Published online: 22 January 2022
© The Author(s), under exclusive licence to Springer-Verlag GmbH Germany, part of Springer Nature 2021

Abstract

The pressure and dependence on coastal aquifers are on the rise in many parts of the globe. These lead to overexploitation, aggravated levels of groundwater pollution, and seawater intrusion. Integrated analyses can create holistic insights into the quality and the vulnerability of aquifers to seawater intrusion. In this study, Mombasa North coast's coastal aquifer was characterized by integrating multiple approaches—GALDIT overlay index, seawater intrusion groundwater quality index GQI_{SWI} , total hardness, water quality index (WQI)—and the results were further explored and interpreted with geospatial analysis techniques. The study suggests that the predominant water type in areas under moderate or high vulnerabilities to seawater intrusion is the Na-Cl water type. However, similar Na-Cl water types can produce a range of total hardness from soft to hard. GQI_{SWI} classification can be used to narrow down the observations from Stuyfzand's TH-based classification system. In the aquifer studied, the results of the GALDIT overlay index, a weighted aggregation of intrinsic parameters contributing to seawater intrusion, show that 29%, 59%, and 12% of the aquifer have low, moderate, and high vulnerabilities, respectively. The GQI_{SWI} analysis indicates that the groundwater is largely brackish (68%) but saline towards the southern end of the aquifer at 32%. Total hardness values indicate that 67% of the aquifer's coverage falls under the “moderately hard” category. The geodatabase creation introduced in the study provides a template for similar studies and a baseline for future WQI and water quality monitoring. However, temporal studies on chronological timescales are recommended for sustainable management of the aquifer.

Keywords Seawater intrusion · Groundwater pollution, Coastal aquifer · GALDIT method · Water quality index · Total hardness · GIS and remote sensing

Introduction

With more than half of the global population residing and making a living in towns and cities, the sustainability of water supplies is a major concern. This is more pronounced in coastal areas, where net migration is much higher than

Responsible Editor: Xianliang Yi

✉ Temitope Ezekiel Idowu
temitope.idowu@tukenya.ac.ke

¹ School of Civil and Resource Engineering, Technical University of Kenya, P.O Box 52428-00200, Nairobi, Kenya

² Center for Applied Coastal Research, University of Delaware, Newark, DE, USA

³ Department of Geoinformation & Earth Observation, Technical University of Kenya, Nairobi, Kenya

⁴ Inst. for Basic Sci. Tech & Innovation-Pan African University at JKUAT, Juja Main Campus, Juja, Kenya

⁵ Department of Physics, Jomo Kenyatta University of Agriculture and Technology, Juja, Kenya

⁶ Regional Centre for Mapping of Resources for Development, Nairobi, Kenya

⁷ Institute of Urban Environment, Chinese Academy of Sciences, Xiamen 361021, China

⁸ Department of Civil and Environmental Engineering, Federal University of Technology Akure, Akure PMB704, Nigeria

the national averages (Wong et al. 2014). Therefore, groundwater has emerged as a vital water resource for meeting the domestic, industrial, agricultural, and environmental demands owing to its relatively consistent yield of good-quality water. In many coastal regions, already scarce fresh groundwater resources are under an unprecedented amount of stress from different drivers and pressures, including urbanization and land-use change (Nlend et al. 2018; Idowu et al. 2020; Ajibade et al. 2021), population growth (Okello et al. 2015), increased domestic and commercial demand, and climate change (Aladejana et al. 2020; Stein et al. 2020). Fresh groundwater resources are dynamic in nature and are affected by these factors; hence, monitoring and conserving aquifers are crucial for sustainable groundwater management.

In coastal settlements, demographic change has intensified the rate of groundwater abstraction and dependence on groundwater, thereby resulting in groundwater vulnerability to depletion and pollution. When groundwater levels in aquifers deplete faster than they can recharge, it results in seawater intrusion (SWI). The direct negative impact of aggravated SWI is that it diminishes the quality and the availability of the water for potable use and other needs. Several studies in different parts of the globe have shown that increased levels of seawater intrusion have far-reaching adverse impacts on humans and the environment. It reduces groundwater quality below the quality thresholds for drinking water (Naseem et al. 2018; Mahammad and Islam 2021), negatively impacts irrigation practices and agriculture (Heydarirad et al. 2019; Sarkar et al. 2021), proves detrimental to human health and living conditions (Siyal 2018; Shammi et al. 2019), and causes adverse effects on coastal ecology and freshwater marsh (Herbert et al. 2018; Siyal 2018) and a host of other undesirable effects.

The theoretical background on seawater intrusion can be found in many studies (Verruijt 1968; Darnault and Godinez 2008; Vengadesan and Lakshmanan 2019). Sea level rise has been identified as one of the factors impacting sea water intrusion (Idowu and Home 2015; Ketabchi et al. 2016; Vu et al. 2018). More exhaustive details on the anthropogenic-driven factors including land-use change and climatic factors impacting the seawater intrusion (SWI) are provided in many published texts (Bear et al. 1999; Barlow 2003; Kogo et al. 2019; Kumar et al. 2019). The multifaceted nature and wide range of factors affecting SWI and the quality of a coastal aquifer make it a dynamic problem. For instance, hydrogeological factors are relatively stable over decades and sometimes centuries, but land use land cover changes are not.

Fresh groundwater quality assessments have often taken a multi-approach where two or more techniques are combined in one study (Krishna-Kumar et al. 2015; Bouderbala et al. 2016; Akoteyon et al. 2018). The focus of groundwater quality assessments depends on the objectives, e.g., irrigation

purpose, municipal use, and most commonly drinking/potable water suitability. One of the widely used techniques applied for drinking water purposes is the Water Quality Index (WQI) where the water quality in the aquifer of interest is assessed against known water quality standards like the World Health Organization (WHO) guidelines and national standards (Ketata-Rokbani et al. 2011). Several studies have applied the WQI either singly or in combination with other analytical techniques (Alastal et al. 2015; Krishna-Kumar et al. 2015; Bouderbala et al. 2016; Akoteyon et al. 2018; Hamlat and Guidoum 2018).

Groundwater vulnerability assessments take on three broad approaches—statistical, process-based, and index/overlay methods (Al-Abadi 2017). In the case of index/overlay methods, factors known to play influential roles on pollutant movement are mapped, assigned weights, and importance ratings based on significance to the pollutant movement. Typical examples of these factors include geology, hydraulic conductivity, slope, and soil type. These factors are then overlaid and a resultant vulnerability index map that aggregates the impact of all the factors is obtained. The groundwater vulnerability map obtained is usually qualitative and specific to the study area. Groundwater vulnerability is described as either intrinsic or specific, where intrinsic vulnerability, is based on the physical attributes of environmental factors while specific vulnerability factors are concerned with the transport behavior of the contaminant or group of contaminants through the porous medium (Witkowski et al. 2014). Hence, most index and overlay methods measure intrinsic vulnerabilities.

Some existing overlay methods include DRASTIC (Aller et al. 1987), SINTACS (Civita 1994), GOD (Foster 1987), AVI (Stempvoort et al. 1993), EPIK (Doerfliger and Zwahlen 1997) the ISIS (Civita and Regibus 1995), and the GALDIT index (Chachadi and Lobo-Ferreira 2005; Lobo-Ferreira et al. 2005). Comparisons of the performance of these methods have been done in many studies as in the case of Luoma et al. (2017), where GALDIT, AVI, and SINTACS were compared in a single study, or Bouderbala et al. (2016) where AVI, GALDIT, and WQI were utilized for assessing the quality and the vulnerability of the coastal aquifer in Tipaza, North Algeria, and a comparison between GALDIT and DRASTIC indices in Kapas Island, Malaysia (Kura et al. 2015). Commonly used indices are DRASTIC, for determining the vulnerability of groundwater to anthropogenic pollution from surface sources, and SINTACS—a modified DRASTIC method—with more weight-strings and additional factors associated with human activities and watercourses. However, the application of DRASTIC and SINTACS to coastal aquifer studies is limited because they do not account for seawater intrusion contamination. Hence, the GALDIT index which utilizes a similar system of rating and weightages to DRASTIC, but focuses more on detecting

the vulnerability of a coastal aquifer to SWI was developed (Chachadi and Lobo-Ferreira 2005; Lobo-Ferreira et al. 2005).

Alongside the GALDIT overlay index, analytical approaches focusing on seawater intrusion have also been developed. Typical examples include the seawater mixing ratios (Lee et al. 2015); Stuyfzand classification based on total hardness (Stuyfzand 1993); and a robust improvement on seawater mixing ratio developed by Tomaszewicz et al. (2014), known as the seawater intrusion groundwater quality index GQI_{SWI} . GQI_{SWI} helps generate a representative seawater intrusion index not only based on seawater mixing ratio but also piper analytical system. With the impressive advances in GIS and geospatial analysis, the point values obtained from these analyses can be spatially shown as maps using spatial interpolation techniques.

Many of the groundwater quality and vulnerability studies have either leaned more towards geospatial analyses/overlay indices than statistical/analytical analyses (Eguaroje et al. 2015; Kura et al. 2015; Bouderbala et al. 2016; Ezekiel et al. 2016; Luoma et al. 2017; Seenipandi et al. 2019; Wei et al. 2021) or vice versa (Bouderbala 2017; Idowu et al. 2017; Aminiyani and Aminiyani 2020; Hajji et al. 2020). Some studies managed to create an even balance between geospatial and statistical analyses but only covered narrower scopes (Ayed et al. 2018; Vaiphei et al. 2020). There is also a growing interest in the application of machine learning techniques to water quality and seawater intrusion studies (Etsias et al. 2020; Bordbar et al. 2021; El-Bilali et al. 2021). Although the application of machine learning algorithms like artificial neural network (ANN) and support vector machine (SVM) in coastal groundwater is currently in its fledgling stage, this research direction is likely to expand in the nearest future.

Coastal groundwater pollution studies require an integrated approach due to the multi-faceted nature of the environmental and anthropogenic-driven processes impacting the quality and pollution status of the groundwater. The application of a single approach to the study of groundwater geochemistry tends to produce unreliable or skewed results (Werner et al. 2013). Therefore, the main aim of this study was to integrate overlay index and analytical and geospatial techniques—three different approaches to coastal groundwater studies—and use the aggregated results for creating a holistic understanding of the water quality and SWI status of a coastal aquifer. The water quality focus is on the suitability of the groundwater for drinking water purposes based on established standards. Furthermore, little emphasis has hitherto been placed on the role of efficient geodatabases in creating detailed and balanced spatio-statistical analyses of coastal aquifers. Hence, the secondary objective of this study was to provide a transferable template for the creation and management of geodatabases used in the study of coastal aquifers. In this study, the GALDIT overlay index

was combined with GQI_{SWI} , WQI, the Stuyfzand classification analytical approaches, and geospatial analyses for assessing the effect of seawater intrusion and water quality extent in the coastal aquifer of Mombasa North Coast. The combination of these approaches can be an effective and consistent way of assessing the amount and extent of seawater intrusion, and the water quality condition of the aquifer in the bid to meet water quality standards. The methodologies introduced in this study are not location specific and therefore applicable to other areas for short and long-term monitoring of coastal aquifers. The findings of the study provide insights to environmental managers and policy makers for sustainable aquifer management practices like protecting susceptible areas and implementing adaptation plans for coastal aquifers.

Study area

The study area is in the northern part of Mombasa, Kenya, covering an area of 74.2 km² and lying between latitudes 3° 95" and 4° 07" and longitudes 39° 68" and 39° 72" south of the equator and east of the Greenwich meridian, respectively. It is bounded by the Indian Ocean on the East, creeks on the northern and southern ends, and elevated hills on the west (Fig. 1). A 2019 national census shows that it has a combined population of 508,507 encompassing two administrative sub-counties—Kisauni and Nyali (KNBS 2019). This is a 34% population increase in the last decade where the combined population in 2009 was 380,055 (KNBS 2010). The climate of the study area is largely tropical and characterized by high humidity and warm temperatures. The difference between the day and night temperatures could range from 6 to 8 °C with temperatures reaching as high as 30 °C from January to March (the warmer months) while night temperatures hover around 20 °C throughout the year (Kenya Coast 2011). Monsoons and the passage of the biannual intertropical convergence zone (ITCZ) also impact the climate of the area with the north-eastern and south-eastern monsoons experienced from January to March and June to October, respectively. Most of the rainfall is experienced between these two monsoon winds with annual precipitation averaging 1072.7 mm (Climatemps 2017).

The geological formation is of the Pleistocene age where the coastal belt was formed as a result of sea-level fluctuations and is mainly composed of sedimentary deposits, corals, coral breccia, and wind-blown sands (Caswell 2007). The lithology is heterogeneous, comprising sandstone, limestone, and shale while the geomorphology is characterized by sandy beaches, creeks, rock-strewn shores, coral reefs, and muddy tidal flats (Abuodha 2004). The topography is relatively flat with low elevations mostly below 42 m above mean sea level (MSL), except for the elevated Nguu Tatu

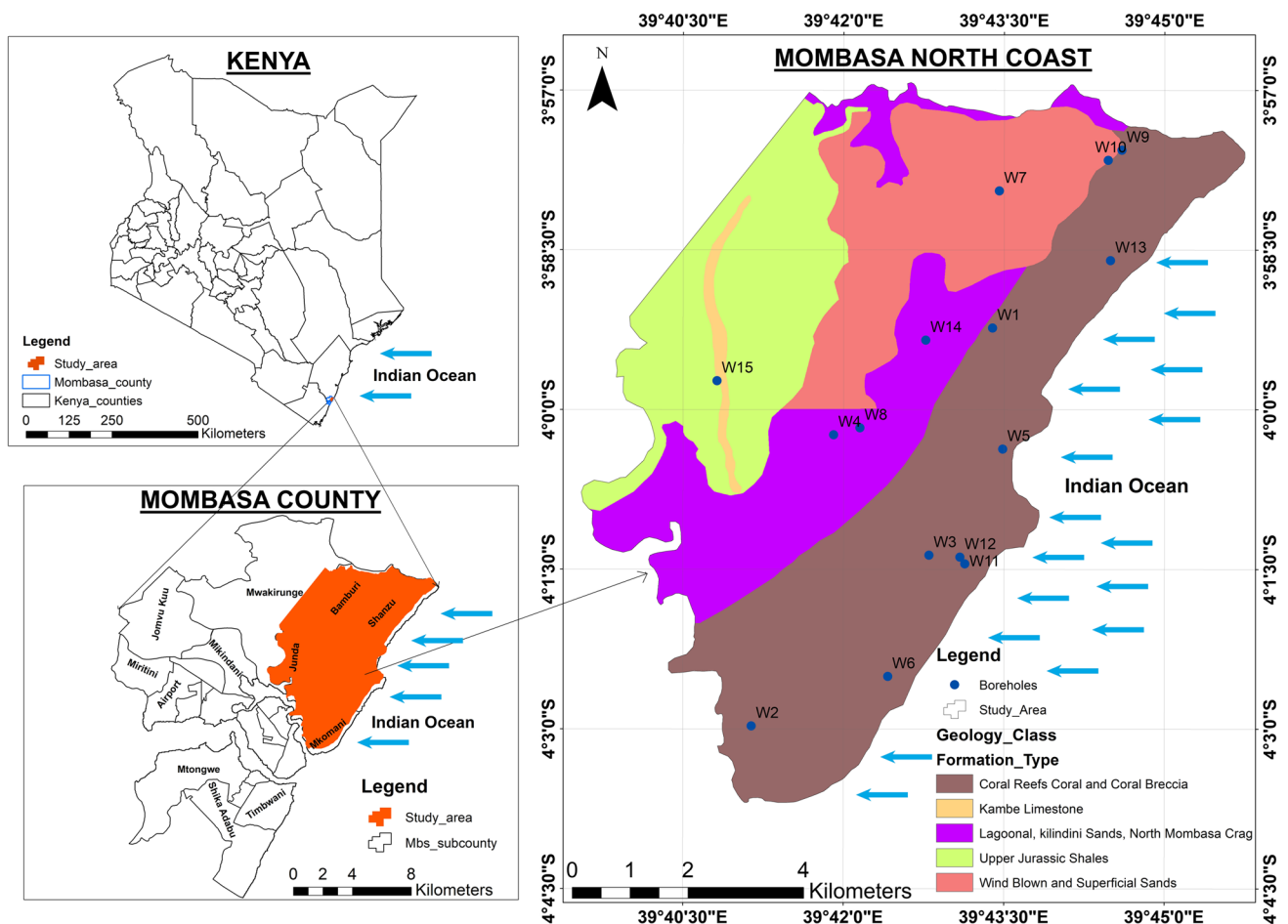


Fig. 1 Study area

hills located on the western end of the study area (Idowu et al. 2017). The study area's aquifer is unconfined and is part of the 15,000 km² transboundary Karoo sedimentary aquifer located between the southern and northern coasts of Kenya and Tanzania, respectively (Igrac 2017). The water table in the study area is relatively shallow but varies widely across the study area (Idowu 2017). The major sources of piped freshwater include the Marere and Mzima springs, Tiwi boreholes, and Baricho wellfields all of which are located outside the administrative boundaries of the study area. A recent study highlights that piped systems only supply a quarter of the city's daily water needs and the rest are being supplied by groundwater from private boreholes and wells (Kithiia and Majambo 2020). This implies that groundwater is the principal source of freshwater in the city and the dependence on groundwater is rapidly increasing due to the exponential population increase. The impact of this continued dependence on groundwater has largely been in the form of increased pollution. An extensive review of the groundwater of the study area describes the recent pollution-related studies and highlights the presence of high

groundwater salinity which varies seasonally, and is usually more severe in the drier months (Idowu and Lasisi 2020).

Methodology

Data description

Geological information, water quality parameters from the field, laboratory test results, and geospatial data were obtained in achieving the objectives of the study. The geological data were obtained from the Mines and Geology department of the Ministry of Environment and Natural Resources of the study area (Caswell 2007). The hydrochemical data is based on extensive post-monsoon groundwater quality data. Post-monsoon data was considered because groundwater recharge is relatively lower and abstraction rates are higher due to the absence of rainfall and rainwater. The data include the groundwater heads above mean sea levels determined by subtracting static groundwater level measurements obtained using water level meters from the

digital elevation model (DEM) of the study area. Other parameters include in situ measurements of the electrical conductivity (EC), total dissolved solids (TDS), and pH all measured using a portable Hanna HI 99,300 conductivity meter. Subsequently, the major cations and anions were analyzed in the laboratory from the samples obtained in the boreholes and wells. The concentrations of cations Na^+ and K^+ were determined using the flame emission spectroscopy while Mg^{2+} and Ca^{2+} concentrations were determined using the flame atomic absorption spectroscopy. The anions HCO_3^- and SO_4^{2-} concentrations were determined using acidimetric neutralization, and turbidimetric method using a spectrophotometer, respectively, while and Cl^- concentrations were determined through the colorimetric determination of chlorine using mercuric thiocyanate, ferric ion, and spectrophotometer.

The importance of an orderly geodatabase for scientific data analysis is rarely stressed, yet it considerably improves the performance and ease of data management. In ArcGIS, creating efficient file geodatabases has been observed to improve versatility, and re-usability of datasets, ease of

migration, and editing and also enables customizable storage configuration, easy updates to spatial indices, and data compression (Childs 2009). Hence, in this study, a central geodatabase was created comprising the field data such as the groundwater levels, electrical conductivity, and total dissolved solids values, laboratory data comprising the analyzed cations and anions, and the secondary data obtained from a wide variety of sources using the ArcGIS 10.2 version (Fig. 2). The geodatabase stores the shapefiles containing the spatial attributes of the sampled boreholes and wells such as location, water level measurements, DEM values, and the in situ and laboratory-tested water quality information shown in Fig. 2. The geodatabase was used for the spatial and water quality analyses that are detailed in the remaining parts of this section. Subsequently, smaller sub-databases were created for each index for ease of carrying out the spatial analyses (Fig. 2).

The geospatial analysis of the results of each analytical technique was explored using spatial interpolation techniques. The techniques were used for creating raster surface maps from the point data resulting from the analytical

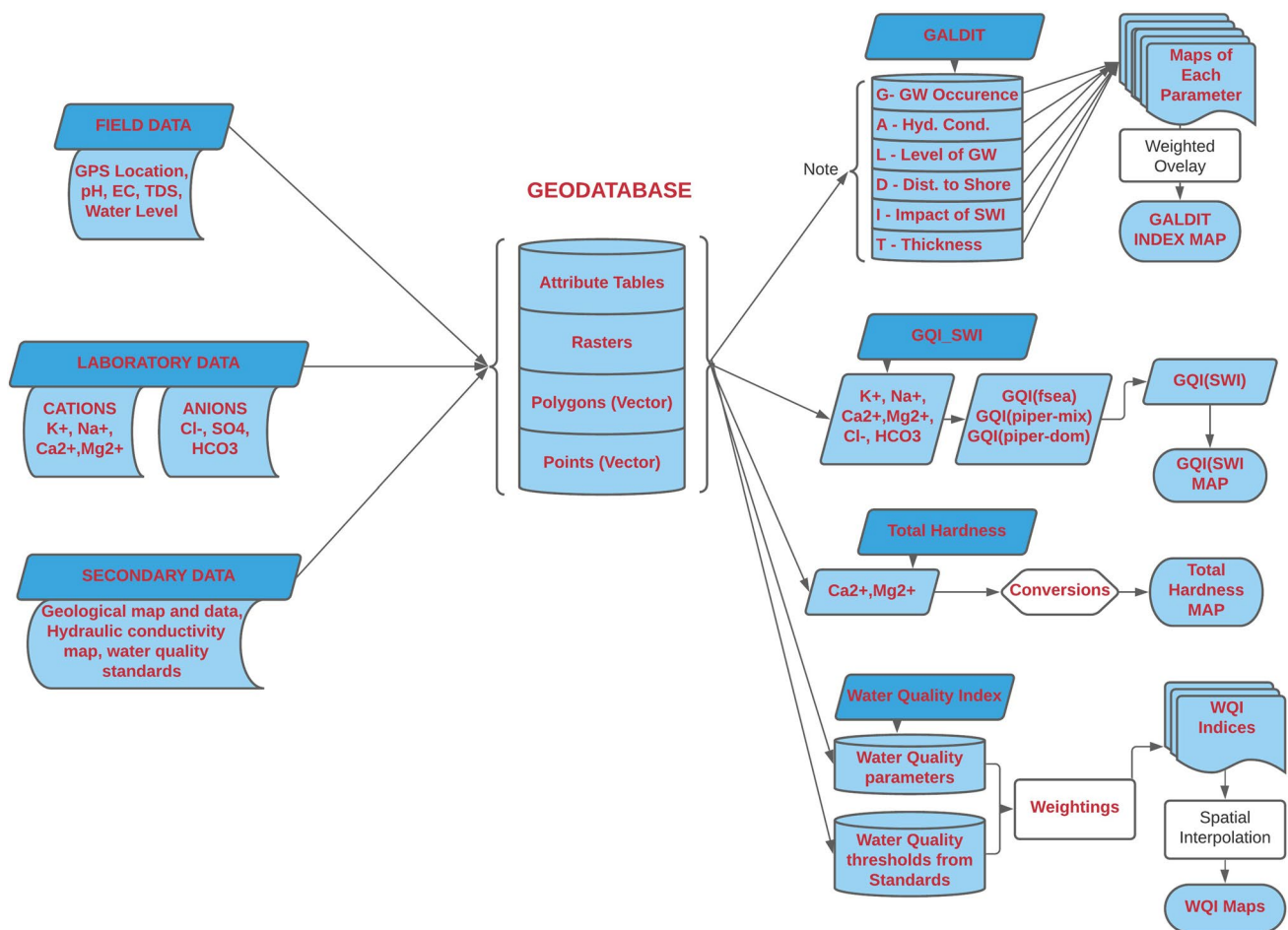


Fig. 2 Schematic representation for the file geodatabase creation workflow

techniques. The two techniques used are the Inverse distance weighted (IDW) interpolation and kriging interpolation technique. The IDW technique is a deterministic form of interpolation where data from known scattered points are used to estimate the data for the unknown points within the data frame using a weighted average and local neighborhood (ESRI 2019). Kriging, a spatial interpolation method based on geostatistics, is an exact interpolator where interpolated values are the best linear unbiased predictors (Karami et al. 2018; CPH 2021). More detailed explanations of these techniques can be found in the literature (Mitas and Mitasova 1999; Karami et al. 2018; ESRI 2019). In this study, it was observed that the IDW method produced better results for the point data with a relatively smaller range of standard deviation values while the kriging method was more effective for the point data with relatively wide ranges of standard deviation value. The cartographic capacity of the GIS was fully employed in creating the final maps from the raster surfaces created thereby helping to create comprehensive, visual and spatial impressions of the results. The application of spatial interpolation techniques for groundwater characterization has also been adopted in previous studies (Ketata-Rokbani et al. 2011; Trabelsi et al. 2016).

GALDIT overlay index

The GALDIT overlay index, based on a numerical ranking procedure is an open-ended model specifically developed to assess the vulnerability of coastal aquifers to seawater intrusion. It was initially developed and improved in the early 2000s (Chachadi and Lobo-Ferreira 2001a, b, 2005; Lobo-Ferreira et al. 2005). The method focuses on the use of hydrological, hydrogeological, and geomorphological characteristics of an aquifer for assessing its intrinsic vulnerability to seawater intrusion. The method is a mapping approach that involves developing comparable maps of six measurable parameters identified as most critical in determining the vulnerability of a coastal aquifer to saline pollution. The ease of data collection and the simplicity of the approach have led to its wide application in many studies around the globe (Sophiya and Syed 2013; Bouderbala et al. 2016; Ezekiel et al. 2016; Chang et al. 2019; Amarni et al. 2020). The GALDIT acronym is derived from the first letters of the six main factors determining the impact of SWI on a coastal aquifer—“Groundwater occurrence, Aquifer hydraulic conductivity, Level of groundwater above MSL, Distance from shore, Impact of the existing status of SWI, and the Thickness of aquifer.” Further details on the conceptual and theoretical frameworks of the technique can be found in the literature (Chachadi and Lobo-Ferreira 2005; Lobo-Ferreira et al. 2005). Beyond the conceptual framework, several studies

have also modified or optimized the technique to suit the specific study area or for better performance (Bordbar et al. 2019; Barzegar et al. 2021; Wei et al. 2021). In this study, the GALDIT factors were determined based on the theoretical frameworks (Chachadi and Lobo-Ferreira 2005; Lobo-Ferreira et al. 2005), the location-specific observations, and insights from previous related studies on the study area (Munga et al. 2006; Ezekiel et al. 2016). The factors and how they are determined for the study area are briefly described below.

Groundwater occurrence (G)

The groundwater occurrence describes the aquifer type—confined, unconfined, leaky-confined, or possessing geological boundaries. Confined aquifers are considered the most vulnerable due to the inherently high pressure in the water and relatively high cones of depression created during pumping. However, the characteristic lower pressures in unconfined aquifers also imply that the hydrodynamic resistance of the freshwater to SWI will be lower, hence making it more vulnerable (Sundaram et al. 2008). The parameter G was obtained from the geological reports and maps of the study area (Caswell 1954a, b, 2007). The maps were georeferenced, and the geology of the study area was clipped and processed from the georeferenced maps. Subsequently, the raster generated was stored in the sub-database for GALDIT indices (Figs. 2 and 3).

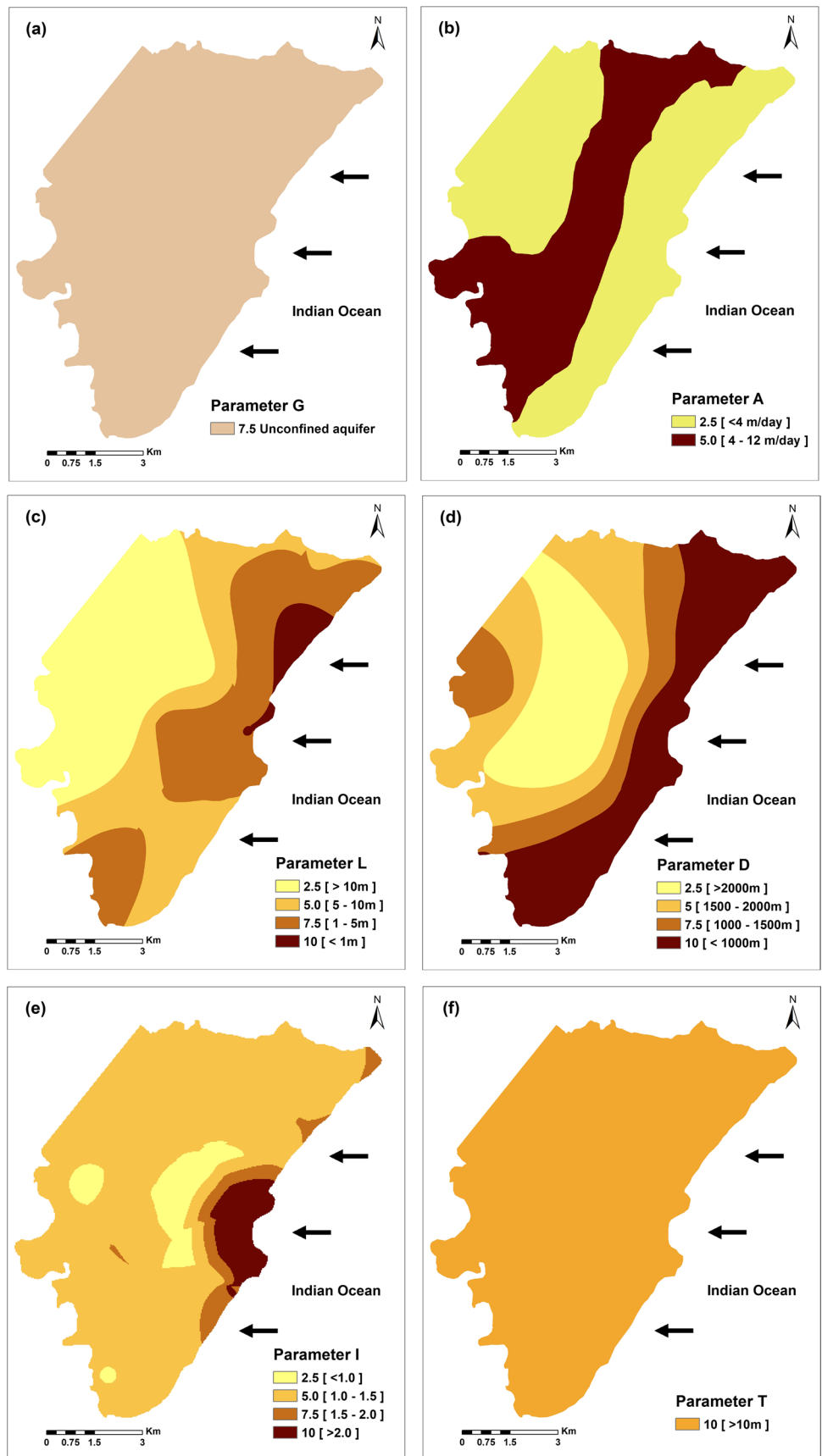
Aquifer hydraulic conductivity (A)

The hydraulic conductivity “k” of the aquifer measures the rate at which water moves by gravity through the saturated zone within the aquifer. High *K* values imply a greater flow rate per unit time, leading to wider cones of depression during abstraction and thereby, increasing the likelihood of SWI (Sophiya and Syed 2013). Parameter A for the study area was obtained from the literature (Munga et al. 2006; Ezekiel et al. 2016).

Level of groundwater above mean sea level (L)

This is one of the most significant factors influencing the SWI in a coastal aquifer. The height of the groundwater above MSL provides a countering freshwater hydraulic pressure against seawater. Hence, the lower the groundwater level, the lower the hydraulic pressure and the higher the risk of intrusion. This phenomenon is illustrated by the Ghyben-Herzberg equation (Verruijt 1968). Parameter *L* for this study was determined by setting the static water levels measured against the study area’s Digital Elevation Model (DEM) and determining the difference.

Fig. 3 a–f GALDIT parameter maps for the coastal aquifer of Mombasa North coast, Kenya



Distance from shore (D)

This is the distance inland in the direction perpendicular to the seawater body. Areas of higher proximities to the shore or creeks are more susceptible to SWI. This parameter was determined from the shapefile map of the study area using the NEAR tool of the spatial analyst on ArcGIS 10.2.

Impact of the existing status of SWI (I)

Several indices indicative of seawater intrusion are used for determining this parameter and are highlighted in Klassen et al. (2014), the most widely used being Simpson's ratio or Revelle's coefficient. The coefficient is a ratio of chloride ions to bicarbonate ions contained in a groundwater sample (Sudaryanto and Nailly 2018). Hence, in this study, the "I" factor was determined for each sampling point by computing the ratios of chloride and bicarbonate ions.

Thickness of the aquifer (T)

This is the saturated thickness of the unconfined aquifer which also influences the extent of the impact of SWI. A larger thickness makes the aquifer more prone to SWI (Chang et al. 2019). As with parameter G, the thickness of the aquifer was obtained from the geological reports and maps of the study area (Caswell 1954a, b, 2007). The information shows that the unconfined aquifer is heterogeneous in nature comprising sandstone, limestone, and shales extending up to 100 m below the surface (Caswell 2007).

The overall GALDIT index vulnerability map was based on decision criteria where each GALDIT parameter was assigned weightages based on Chachadi and Lobo-Ferreira (2005). The ranges of values of the importance ratings were determined based on the uniqueness of the study area as shown in Table 1. The numerical rankings range from 0 to 10, where 2.5, 5.0, 7.5, and 10 represent very low, low, medium, and high vulnerabilities, respectively. The decision criteria are represented by Eq. 1 as introduced by Chachadi and Lobo-Ferreira (2005).

Table 1 Summary of the GALDIT parameters, weightages, rates, and importance ratings

Parameter	Weightages	Indicator variables		Importance ratings
		Class	Range	
<i>Groundwater occurrence (G)</i>	1	Confined aquifer		10
		Unconfined aquifer		7.5
		Leaky confined aquifer		5
		Bounded aquifer		2.5
<i>Aquifer hydraulic conductivity (A) (m/day)</i>	3	High	> 40	10
		Medium	12–40	7.5
		Low	4–12	5
		Very low	< 4	2.5
<i>Level of groundwater above mean sea level (L)</i>	4	High	< 1	10
		Medium	1–5	7.5
		Low	5–10	5
		Very low	> 10	2.5
<i>Distance from shore (D) in meters</i>	4	High	< 1000	10
		Medium	1000–1500	7.5
		Low	1500–2000	5
		Very low	> 2000	2.5
<i>Impact of the existing status of SWI (I)</i> [Simpson's ratio]	1	High	> 2	10
		Medium	1.5–2	7.5
		Low	1.0–1.5	5
		Very low	< 1.0	2.5
<i>Thickness of the aquifer (T) in meters</i>	2	High	> 10	10
		Medium	7.5–10	7.5
		Low	5–7.5	5
		Very low	< 5	2.5

$$GALDIT_{index} = \frac{\sum_{i=1}^6 (W_i R_i)}{\sum_{i=1}^6 W_i} \tag{1}$$

where W_i and R_i are the weightages and the importance ratings of the i^{th} GALDIT parameters, respectively. Based on Eq. 1, the final vulnerability map is scaled from 0 to 10 where < 2.5, 2.5 – 5.0, 5.0 – 7.5, and 7.5 – 10 represent very low, low, medium, and high vulnerabilities, respectively (Lobo-Ferreira et al. 2005).

Maps based on the importance ratings of these six parameters were created on ArcGIS 10.2. Subsequently, the six maps were overlaid according to the weightages, using the *weighted sum* tool in the spatial analyst toolbox to obtain the aggregated GALDIT vulnerability map.

Seawater intrusion groundwater quality index

One of the most widely used analytical methods for detecting and assessing the impact of seawater on coastal groundwater is the fresh/seawater mixing equation (Lee et al. 2015; Idowu et al. 2017; Alfarrak and Walraevens 2018). However, it has its limitations and a major one is that it only considers chloride ions as an indicator for SWI. SWI is a dynamic process that is not limited to the presence of chloride ions alone. Hence, a study by Tomaszekiewicz et al. (2014) attempted to address this limitation by incorporating other ions in the analytical process. This was achieved by improving on the fraction of seawater (f_{sea}) equation also known as the seawater mixing ratio (Appelo and Postma 2005; Lee et al. 2015) and further developing an analytical framework with equations and for assessing the impact of SWI based on four cations— Ca^{2+} , Mg^{2+} , Na^+ , K^+ , and two anions— HCO_3^- , Cl^- generally used to create piper plots (Tomaszekiewicz et al. 2014). This approach, known as SWI groundwater quality index (GQI_{SWI}), is expressed by Eqs. 2 to 6. The parameters were converted from mg/L to meq/L using the ASCE SI unit conversion (ASCE 2012).

$$f_{sea} = \frac{m_{cl(sample)} - m_{cl(freshwater)}}{m_{cl(seawater)} - m_{cl(freshwater)}} \tag{2}$$

f_{sea} is also referred to as the seawater mixing ratio (SMR)

$$GQI_{f_{sea}} = (1 - f_{sea}) \times 100 \tag{3}$$

$$GQI_{piper(mix)} = \left(\frac{Ca^{2+} + Mg^{2+}}{Total\ Cations} + \frac{HCO_3^-}{Total\ Anions} \right) \times 50 \text{ (in meq/l)} \tag{4}$$

$$GQI_{piper(dom)} = \left(\frac{Na^+ + K^+}{Total\ Cations} + \frac{HCO_3^-}{Total\ Anions} \right) \times 50 \text{ (in meq/l)} \tag{5}$$

$$GQI_{SWI} = \frac{GQI_{piper(mix)} + GQI_{f_{sea}}}{2} \tag{6}$$

A global analysis of different water types by Tomaszekiewicz et al. (2014) in relation to GQI_{SWI} shows the typical range of values for freshwater, mixed, saline, and seawater (Table 2).

In this study, the groundwater is classified into different water types based on the computed GQI_{SWI} . Furthermore, the $GQI_{piper(mix)}$ and $GQI_{piper(dom)}$ were subjected to a hierarchical analytical framework (Tomaszekiewicz et al. 2014). The framework identifies the water type according to the piper diagram-based domains categorized as I, II, III, IV, V, and VI denoting Ca- HCO_3 , Na-Cl, mixed Ca-Na- HCO_3 , mixed Ca-Mg-Cl, Ca-Cl, and Na- HCO_3 water types, respectively (Sarath Prasanth et al. 2012; Mtoni 2013). Domain I waters generally connote freshwater while domain II waters are impacted by salinity which may be due to SWI.

Total hardness

Total hardness (TH) is one of the predominant parameters of interest in assessments related to drinking water quality. It is the measure of the amount of calcium and magnesium ions as components of their respective salts dissolved in water. The effects of the total hardness of the water on human health, and phenomena such as taste, corrosion and scaling, desalination, reuse, and other considerations are well detailed in the WHO’s report on water hardness (WHO 2011). The total hardness of GW can also provide some insights into the nature of the water. The extensive work by Stuyfzand (1986, 1993) produced a classification scheme for water based on the total hardness calculated in meq/L using Eq. 7:

$$TH = 5 \times (Ca^{2+} + Mg^{2+}) \text{ in meq/L} \tag{7}$$

The total hardness values in meq/L obtained were converted into mmol/L. The water type classification according to the total hardness in mmol/L is presented in Table 3.

Table 2 GQI_{SWI} ranges (Tomaszekiewicz et al. 2014)

Water type	GQI_{SWI} based on worldwide literature			Typical GQI_{SWI}	
	Min	Max	Mean	Min	Max
Freshwater	73.5	90.1	82.7	75	100
Mixed groundwater	47.8	79.9	63.4	50	75
Saline groundwater	4.8	58.8	27.5	10	50
Seawater	3.1	9.2	5.8	0	10

Table 3 Water-types based on the total hardness (Stuyfzand 1993)

No	Name	Code	Total hardness (mmol/L)	Natural occurrence in main water type
-1	Very soft	*	0–0.5	F
0	Soft	0	0.5–1	F Fb B
1	Moderately hard	1	1–2	F Fb B Bs
2	Hard	2	2–4	F Fb B Bs
3	Very hard	3	4–8	F Fb B Bs
4	Extremely hard	4	8–16	Fb B Bs S
5	Extremely hard	5	16–32	Bs S H
6	Extremely hard	6	32–64	Bs S H
7	Extremely hard	7	64–128	S H
8	Extremely hard	8	128–256	H
9	Extremely hard	9	> =256	H

Note: F: Fresh; Fb: Fresh – brackish; B: Brackish; Bs: Brackish–salt; S: Salt; H: Hypersaline

Water Quality Index

There is a need to understand the water quality on a spatial scale for effective management of groundwater. In many locations, groundwater is used conjunctively with other water sources for serving multiple needs like drinking, domestic, agricultural, and recreational use. Global guidelines, e.g., the WHO guidelines for drinking water and national standards and Kenya drinking water standards, provide quality thresholds not to be exceeded. WQI is a viable management tool for determining the suitability of a water type for different uses and when combined with geospatial techniques, WQI maps can be generated. WQI maps help to visualize locations of the most and least suitable areas for the criteria being observed e.g. drinking purposes based on its mineral contents (Bouderbala et al. 2016). The information that WQI maps provide can easily be understood by researchers and policymakers alike. This can help guide decision-making and contribute to creating a better understanding of the relationships between groundwater quality and other environmental parameters like groundwater depth and land use land cover (Rizwan and Gurdeep 2010). The concept of WQI is based on comparing the relevant water quality parameters in a location with regulatory standards/guidelines and aggregating all the water quality parameters considered to obtain single indices which represent the overall water quality status (Alastal et al. 2015). The single water quality indices were spatially interpolated to obtain the WQI maps. The maps express the water quality information in simple terms such as excellent, good, or poor water quality (Table 4).

The procedure for computing the WQI involves three main steps (Rizwan and Gurdeep 2010; Ketata-Rokbani et al. 2011; Alastal et al. 2015). The first step involves

Table 4 Classification of the WQI scores (Sahu and Sikdar 2008; Ketata-Rokbani et al. 2011)

WQI	Water type
< 50	Excellent water
50–100	Good water
100.1–200	Poor water
200.1–300	Very poor water
> 300.1	Water unsuitable for drinking purposes

assigning weights to each of the water quality parameters being considered based on their impacts, e.g., on health when drinking water standards are being considered.

In the second step, the relative weight (W_i) of each parameter is computed using Eq. 8:

$$W_i = \frac{w_i}{\sum_{i=1}^n w_i}; \quad (8)$$

where (w_i) is the weight of each parameter, (n) is the number of parameters, and (W_i) is the relative weight.

The third step entails calculating a quality rating scale (q_i) for each parameter using Eq. 9:

$$q_i = \frac{C_i}{S_i} \times 100; \quad (9)$$

where “(q_i) is the quality ranking, (C_i) is the concentration of each chemical parameter in each water sample in mg/L, and (S_i) is the WHO standard for each chemical parameter in mg/L.” Finally, the WQI is determined for each chemical parameter using Eq. 10:

$$WQI = \sum_{i=1}^n W_i \times q_i; \quad (10)$$

where (q_i) is the rating based on concentration if (i^{th}) parameter and (n) is the number of parameters. Computed WQI values are usually categorized into five (Table 5): excellent, good, poor, very poor, and unsuitable for human consumption (Rizwan and Gurdeep 2010; Ketata-Rokbani et al. 2011; Alastal et al. 2015).

In this study, the WQI was assessed based on the World Health Organization (WHO) guidelines for drinking water (WHO 2017) and the Kenya Standards for potable water (KEBS 2015). The Kenya standard defines potable water as one “that is safe and suitable for human consumption” (KEBS 2015). The quality requirements set by the two regulatory bodies for the relevant parameters and their perceived weights based on the significance of their impacts on public health are presented in Table 5.

The choice of the parameters is informed by factors like the importance of the parameter as stipulated in the guidelines, the purpose of the index (human health and suitability

Table 5 The thresholds, weights, and relative weights of each parameter

Parameter	WHO Standard (2017)	Weight (wi)	Relative weight (Wi)	Kenya standard for potable water (2015)	Weight (wi)	Relative weight (Wi)	
TDS	1000	5	0.143	1500	5	0.147	
Hardness	100–500	4	0.114	600	4	0.118	
Cl	250	5	0.143	250	5	0.147	
Na	200	3	0.086	200	3	0.088	
SO ₄	250	5	0.143	400	5	0.147	
pH	6.5–8.5	3	0.086	5.5–9.5	3	0.088	
Mg	100	2	0.057	100	2	0.059	
Ca	300	2	0.057	150	2	0.059	
EC	1500	5	0.143	2500	5	0.147	
K	100	1	0.029	-	-	-	
			$\sum wi = 35$				$\sum wi = 34$

for human consumption), and data availability. The assigned weights on each parameter connote the parameter's significance to the overall quality of water on a scale of 1 to 5. The choice of the weights (w_i) as expressed in Table 5 are largely based on the predominant weights previously used in earlier studies (Ketata-Rokbani et al. 2011; Alastal et al. 2015; Bouderbala et al. 2016; Bouderbala 2017; Chaurasia et al. 2018) and the implications of the parameters to human health as outlined in the WHO guidelines.

Results and discussion

GIS and spatial analysis have played an integral role in environmental assessment and their evolution over the years are well detailed by Goodchild and Haining (2003). The focus of this study is on the application of the GALDIT overlay index, GQI_{SWI} , total hardness, and WQI for an integrated assessment of the groundwater quality and vulnerability to seawater intrusion of a coastal aquifer. Besides the spatial analysis tools used for the GALDIT index-weighted overlays, spatial interpolation techniques were extensively used for creating raster surfaces from the point data resulting from the water quality analyses.

The statistical analysis of the data (Table 6) indicates a wide variation in the groundwater geochemistry of the coastal aquifer. Table 6 shows that the chemical parameters in the groundwater vary widely as indicated by the standard deviation values where the EC, and TDS values are 2410 $\mu\text{S}/\text{cm}$, and 1205 mg/L, respectively. Wide variations are also observed in Na, Cl, K, and SO₄ values. The high standard deviation values imply that the quality and characteristics of the groundwater are heterogeneous and widely different water qualities and vulnerabilities can be experienced from one part of the aquifer to another.

Table 6 Statistical summary of the parameters and major chemical constituents in the coastal aquifer of Mombasa North coast

Parameters	Minimum	Maximum	Mean	Standard deviation (SD)
EC ($\mu\text{S}/\text{cm}$)	480	9516	2934	2410
pH	7.46	8.73	7.81	0.32
TDS (mg/L)	250	4748	1503	1205
HCO ₃ (mg/L)	73.8	189.2	120.2	24
Cl (mg/L)	117.6	279.9	145.4	38.4
Mg (mg/L)	0.85	1.74	1.48	0.24
Ca (mg/L)	0.67	18.44	7.59	5.92
Na (mg/L)	47.44	729.10	247.52	185.67
K (mg/L)	1.74	65.77	11.91	16.13
SO ₄ (mg/L)	78.91	328.92	158.10	71.15

These wide-ranging hydrochemical values are better interpreted using multiple techniques, which help to characterize the groundwater holistically. The rest of this section highlights and discusses the results of the GALDIT Index analysis, GQI_{SWI} , total hardness, and WQI in relation to the water quality and vulnerability to seawater intrusion.

The GALDIT index vulnerability map

The results of the GALDIT overlay index for the Mombasa North coast covering an area of 74.2 km² show varying vulnerabilities to seawater intrusion. The parameters G and T which were obtained from the geological reports and maps of the study area (Caswell 1954a, b, 2007) indicate that the aquifer type is unconfined with varying thickness up to 100 m in some locations, and therefore, the G parameter was assigned an importance rating of 7.5 while the T parameter was assigned the maximum rating of 10. The broad importance rating of parameters G and T do not vary across the

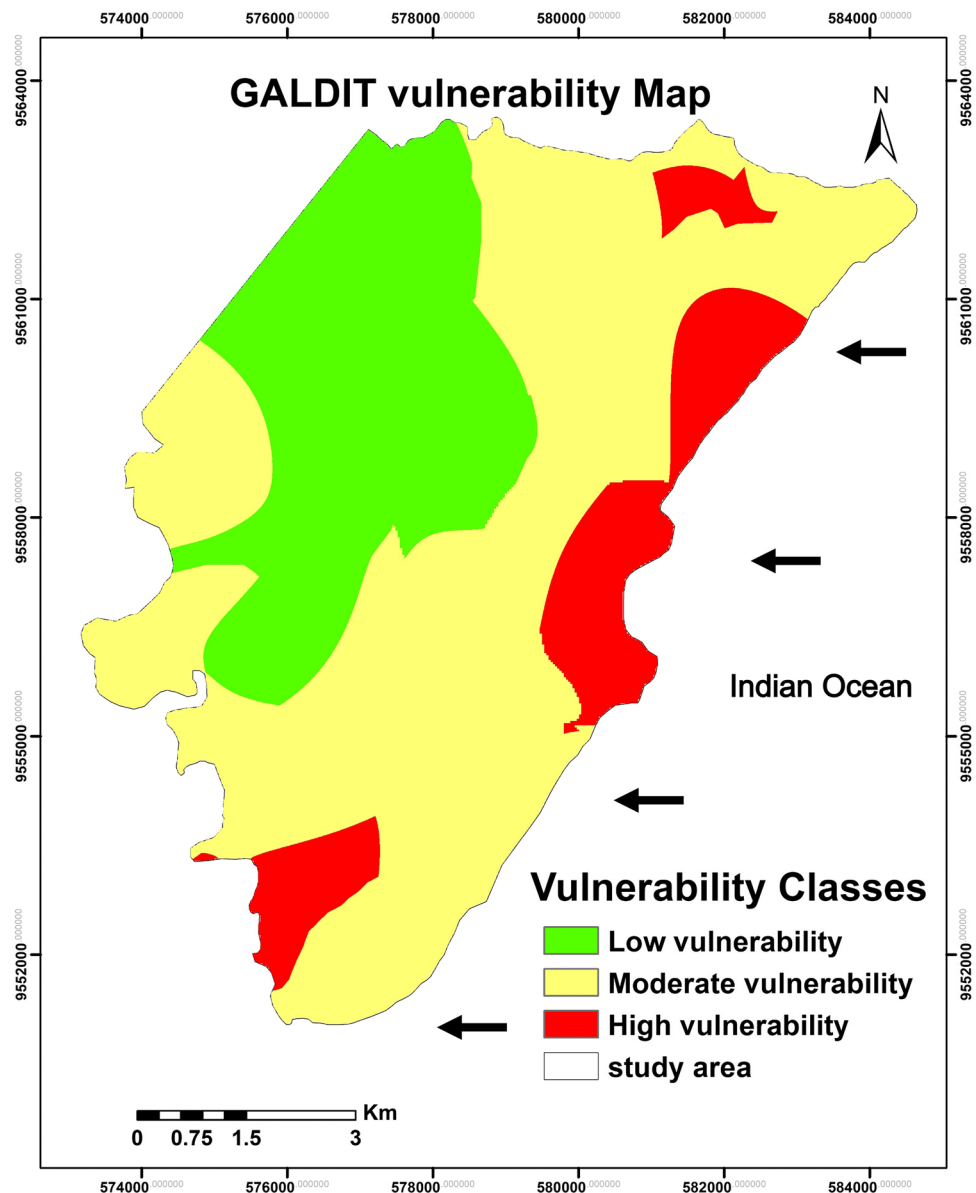
aquifer (Fig. 3a, f); however, they contribute to the weightages and overall vulnerabilities. Removing these parameters from the analysis will lead to errors where disproportionate weightages are assigned to other parameters. For instance, a recent study on the appraisal of the GALDIT index highlighted the sensitivity of the parameters to seawater intrusion, and the two parameters accounted for nearly 20% of the effective weightages (Seenipandi et al. 2019). Hence, the two parameters were included in the overlay analysis.

The hydraulic conductivity of the aquifer (parameter A) was observed to range from < 4 m to 12 m/day (Munga et al. 2006), and therefore, the ratings ranged from 2.5 to 5. It was observed that the static water levels and invariably the height of the groundwater above sea levels varied with seasons in the study area as seen from the dataset. The post-monsoon

groundwater height above the mean-sea level ranged widely from -0.84 to 33.08 m. These values were used to obtain the map for parameter L with importance ratings ranging from 2.5 to 10, depending on the location within the study area. For parameter D (distance to the shore), areas within 1000 m to the seawater body received the highest importance rating of 10 while areas greater than 2000 m were assigned the lowest ratings of 2.5. Finally, Simpson's ratio used for obtaining the parameter I ranged from 0.65 to 3.58 with values < 1.0 being assigned the lowest rating of 2.5 and values > 2 ascribed the highest rating of 10. The maps for each parameter are highlighted in Fig. 3.

The aggregated GALDIT vulnerability map resulting from the weighted overlay of the GALDIT parameter maps is shown in Fig. 4.

Fig. 4 GALDIT vulnerability map for the coastal aquifer of Mombasa North coast, Kenya



The GALDIT overall index map was found to range from 3.83 to 8.33 which indicates that no part of the aquifer is under a “very low vulnerability,” i.e., (<2.5). The computed area coverages for the vulnerability classes are shown in Table 7.

Table 7 shows that almost 60% of the aquifer’s area coverage is under moderate vulnerability while 29% and 12% are experiencing low and high vulnerabilities, respectively. A previous vulnerability study on the aquifer which was based on data obtained at pre-monsoon and the peak of the rainy season shows an equally high percentage of moderate vulnerability to seawater intrusion at 64% and 55% (Ezekiel et al. 2016). However, a closer look at the data trends shows a progressive increase in the low vulnerability area coverage from 13 to 20% observed at pre-monsoon and peak of the rainy season in previous studies to 29% in the current study (post-monsoon). This corroborates previous studies highlighting that rainfall may be responsible for an increase in groundwater recharge which in turn increases the pressure head of freshwater against seawater and hence reduce the impact of SWI (Idowu 2017). In other words, as the rainy season progresses, the aquifer tends to become less

vulnerable to SWI impacts. More importantly, these findings all point to the fact that vulnerability to seawater intrusion is dynamic and varies with seasons.

Seawater mixing index

The GQI_{SWI} values for each groundwater sample represented in Table 8 show there is a wide variation in the water type in the aquifer from a minimum value of 28 (saline water) to a maximum value of 59 (mixed groundwater). A more detailed observation shows that 80% (12) of the samples fall within the range of the mixed water category while the remaining 20% (3 samples) were in the saline water category (Table 8). The surface raster map produced by spatially interpolating the GQI_{SWI} data further confirms that the groundwater is largely mixed, with the saline water mostly concentrated towards the southern parts of the study area close to the ocean (Fig. 5). Furthermore, the GQI_{SWI} map establishes that the aquifer’s groundwater is largely brackish especially in regions towards the northern part of the study area while saline water prevails mostly along the coastlines and towards the southern end of the study area. Hence, Fig. 5 further provides an idea of the spatial distribution of the GQI_{SWI} values which is a more holistic view of the groundwater quality related to seawater intrusion.

The statistical computation of the GQI_{SWI} map is 68% and 32% for the brackish and saline water areas, respectively. This finding compares with an earlier salinity study on the study area based on EC and TDS values, which shows that over 90% of the aquifer’s GW is either saline or brackish (Idowu et al. 2018). Two previous studies that focused on the direction of groundwater flow in the study area (Munga et al.

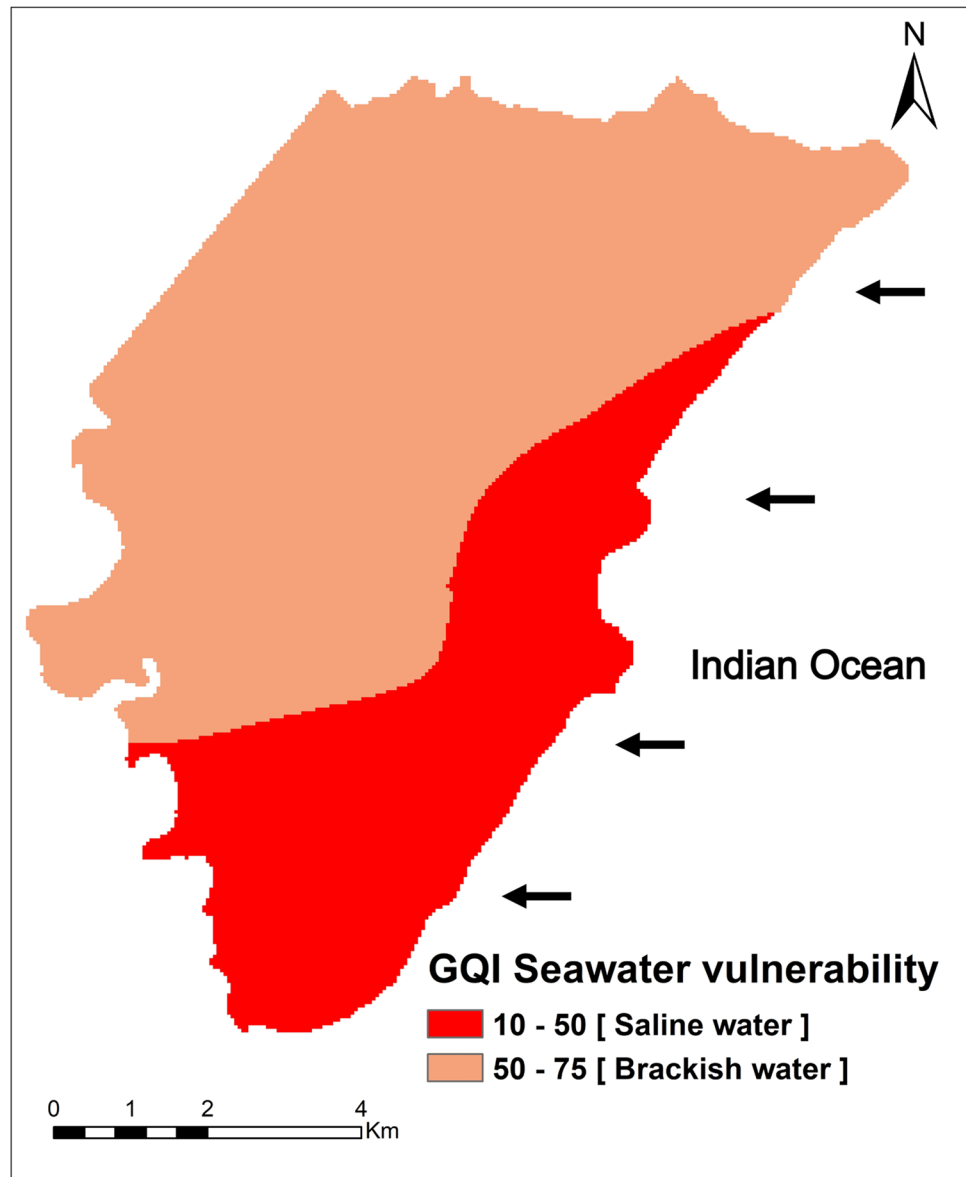
Table 7 Vulnerability categories and their percentage area coverages in the study area

SN	CLASS	Weighted ranges	Area coverage (%)
1	Low vulnerability	<5	29
2	Moderate vulnerability	5–7.5	59
3	High vulnerability	7.5>	12

Table 8 Computed GQI_{piper} and domain category for each sampled location

SN	Sampling location	GQI_{SWI}	Classification based on GQI_{SWI}	$GQI_{\text{piper(mix)}}$	$GQI_{\text{piper(Dom)}}$	Domain (Tomaszkiewicz et al. 2014)
1	Braeburn	55	Mixed GW	18.22	60.17	II
2	Cinema	55	Mixed GW	19.34	59.86	II
3	Krat	55	Mixed GW	15.48	59.50	II
4	M. Hussein	57	Mixed GW	21.07	51.82	II
5	Milele	28	Saline GW	4.68	54.16	II
6	N golf	51	Mixed GW	9.99	57.40	II
7	Redeem	59	Mixed GW	20.46	51.53	II
8	Ruby2	57	Mixed GW	18.59	64.47	II
9	Shimo high	56	Mixed GW	20.73	51.96	II
10	Shimo qtrs	54	Mixed GW	15.94	55.04	II
11	Sos1	48	Saline GW	7.55	56.24	II
12	Sos2	49	Saline GW	9.13	57.45	II
13	Sunsweet	51	Mixed GW	10.41	56.56	II
14	Utange	56	Mixed GW	15.69	62.80	II
15	Vikwatani	52	Mixed GW	11.01	59.27	II

Fig. 5 The GQI_{SWI} map of the coastal aquifer of Mombasa North coast, Kenya



2006; Idowu 2017) report that the flow direction is mainly northwards towards the ocean. Higher water flow rates can decrease the concentration of salts (Hsu 2005). This implies that the constant flow of groundwater in the northward direction may lead to a lower build-up of salts in the groundwater along the flow paths. This might explain why the north and northeastern parts of the study area are characterized by brackish water, which possesses lower concentrations of salts than saline water predominantly concentrated on the southern part of the study area.

The computed $GQI_{\text{piper(mix)}}$ and $GQI_{\text{piper(Dom)}}$ according to Eqs. 4 and 5 are highlighted in Table 8. According to the hierarchical analytical framework for water quality classification by (Tomaszkiewicz et al. 2014), water samples whose values fall within the $GQI_{\text{piper(mix)}}$ range of 0–25 and

$GQI_{\text{piper(Dom)}}$ range of 50–75 are classified as the Na-Cl water type belonging to domain II. It can be observed that for this study, the $GQI_{\text{piper(mix)}}$ are all < 25 and the $GQI_{\text{piper(Dom)}}$ values are all between 50 and 75 (Table 9). Hence, the groundwater is classified as a Na-Cl water type impacted by salinity.

Table 9 presents the aggregation of the GQI_{SWI} , total hardness, and WQI computations as described in the methodology.

Total hardness

According to the WHO guidelines, there are currently no health-based threshold values for hardness in drinking water. However, extremely hard water may precipitate CaCO_3 scales when boiled depending on the pH and alkalinity. On

Table 9 Computed GQI_{SWI} , Total hardness, and WQI values at each sampling location

SN	Sampling location	GQI_{SWI}	Classification based on GQI_{SWI}	Water type based on GQI_{SWI}	Total hardness (mmol/L)	Total hardness classification	WQI (WHO 2017)	WQI class (WHO 2017)	WQI (Kenya standards)	WQI class (Kenya standards)
1	Braeburn	55	Mixed GW	Na-Cl type	1.67	MH	68	Good	59	Good
2	Cinema	55	Mixed GW	Na-Cl type	2.16	H	75	Good	64	Good
3	Krat	55	Mixed GW	Na-Cl type	0.36	VS	53	Good	49	Good
4	M. Hussein	57	Saline GW	Na-Cl type	1.97	MH	68	Good	58	Good
5	Milele	28	Mixed GW	Na-Cl type	0.44	VS	252	Very poor	190	Poor
6	N golf	51	Mixed GW	Na-Cl type	0.88	S	127	Poor	100	Poor
7	Redeem	59	Mixed GW	Na-Cl type	1.82	MH	54	Good	48	Good
8	Ruby2	57	Mixed GW	Na-Cl type	1.02	MH	85	Good	71	Good
9	Shimo high	56	Mixed GW	Na-Cl type	2.60	H	70	Good	59	Good
10	Shimo qtrs	54	Saline GW	Na-Cl type	2.13	H	82	Good	68	Good
11	Sos1	48	Saline GW	Na-Cl type	0.69	S	138	Poor	110	Poor
12	Sos2	49	Mixed GW	Na-Cl type	0.84	S	129	Poor	104	Poor
13	Sunsweet	51	Mixed GW	Na-Cl type	0.81	S	125	Poor	97	Good
14	Utange	56	Mixed GW	Na-Cl type	0.67	S	86	Good	72	Good
15	Vikwatani	52	Mixed GW	Na-Cl type	0.73	S	176	Poor	133	Poor
	Min	28			0.36		53		48	
	Max	59			2.60		252		190	
	Mean	49			1.25		106	Poor	85	Good

MH moderately hard; H hard; VS very soft; S soft

the other hand, “very soft” water may be more corrosive for water pipes due to its low buffering capacity (WHO 2017). The computed total hardness values according to Stuyfzand’s classification system range from 0.36 (very soft) to 2.60 (hard) with a mean value of 1.25 implying moderately hard groundwater (Table 9). It is further confirmed by the GIS-based total hardness map generated from the values (Fig. 6). The area computations for the hardness show that the percentages for very soft, soft, moderately hard, and hard water were 1%, 27%, 67%, and 5%, respectively. This implies that almost 70% of the groundwater in the study area can be considered moderately hard.

Based on Stuyfzand’s classification system, the natural occurrence of moderately hard water could range from fresh to brackish saltwater (Table 4) depending on the geochemical composition of the water. Previous groundwater quality studies in some portions of the study area show that the total

hardness values in mg/L are quite high but are below both the WHO guidelines and Kenya standard values of 500 mg/L and 600 mg/L, respectively (Mwamburi 2013).

Water Quality Index

The WQI values obtained prove that the WHO guidelines are more stringent than the National standard as ranges of 53 to 252, and 48 to 190 were observed in each case, respectively (Table 9). The spatial maps generated from the WQI values (Fig. 7) provide a more holistic understanding of the WQI values. It can be observed that the WQI map based on WHO guidelines shows that more areas fall under the “poor water category.” The area computations for the WQI categories are presented in Table 10.

Fig. 6 Total hardness map for the coastal aquifer of Mombasa North coast based on Stuyfzand’s classification system

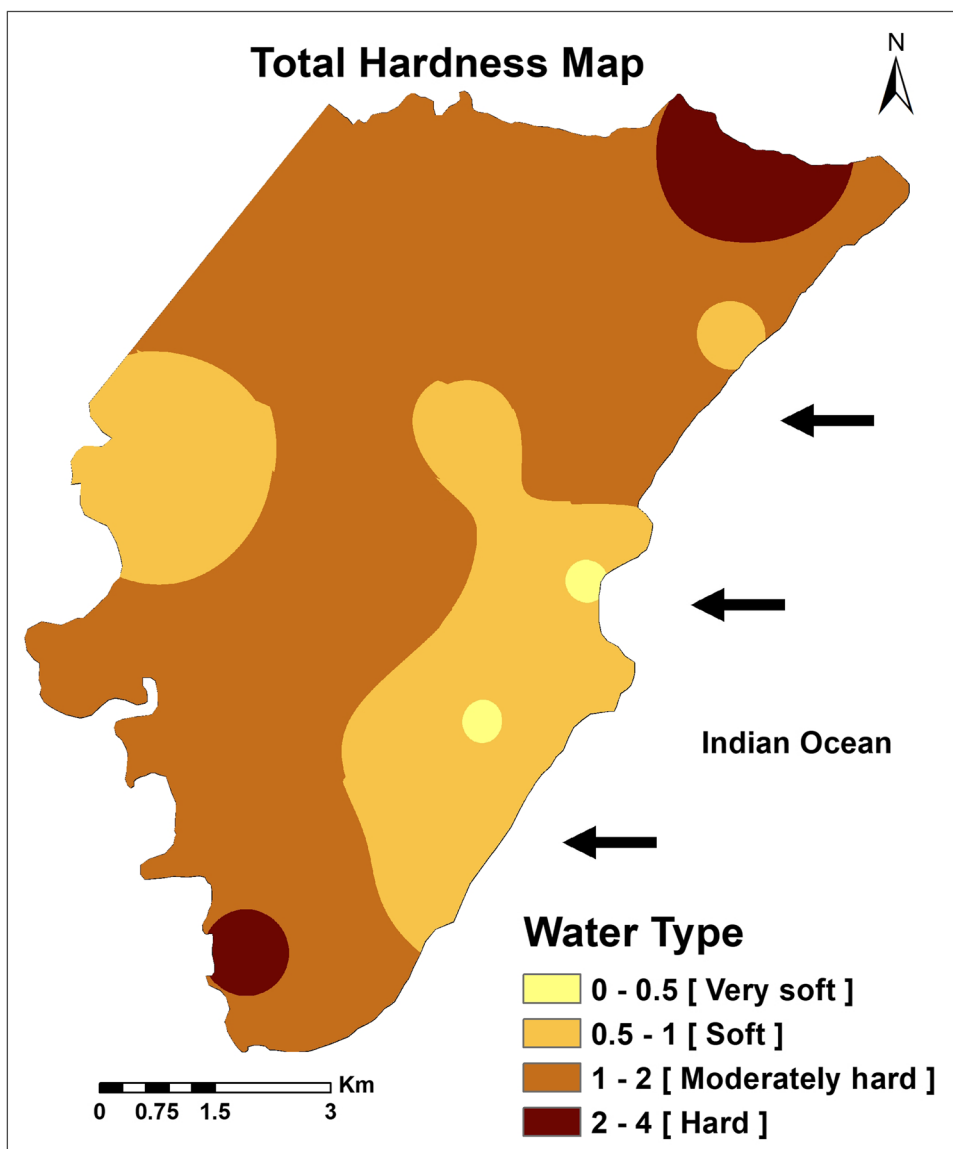


Fig. 7 Water Quality Index maps for the coastal aquifer of Mombasa North coast based on WHO guidelines (a) and Kenya standard (b) for potable water

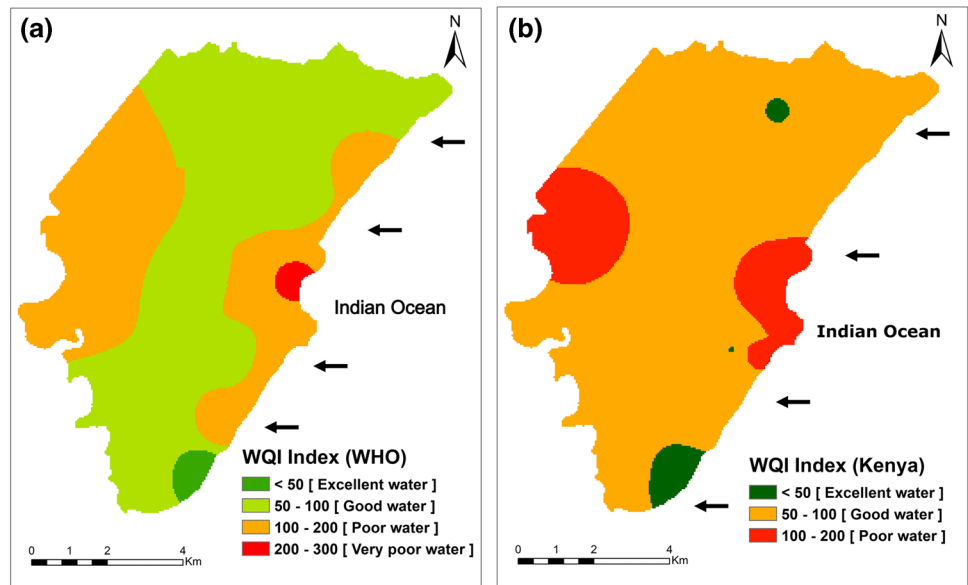


Table 10 The area coverages for each WQI category according to the standards used

WQI classification	WQI (WHO) (%)	WQI (Kenya standards) (%)
Excellent water	1	2
Good water	60	84
Poor water	38	14
Very poor water	1	-
Water unsuitable for drinking purposes	-	-

About 60% and 84% of the aquifer’s coverage are considered good water while 38% and 14% are regarded as poor water for the WHO guidelines and Kenya standards respectively (Table 10). The comparatively high “good water quality” coverage (84%) and low “poor water” coverage (14%) observed for Kenya standards show that the WHO guidelines are more nuanced. Notwithstanding, these findings suggest that studies over multiple timeframes are required to establish a more enduring WQI status of the study area. The indices used for the WQI classification were mainly cations and anions related to SWI pollution, and the GQI_{SWI} analysis has established that the groundwater is the NaCl type; hence, areas with poor water quality are largely impacted by poor salinity due to SWI. The poor water regions on the western part of the study area coincide with the high altitude Ngu-tatu hills known for a high concentration of salts in the groundwater from a previous study (Idowu et al. 2017). However, further studies are needed to ascertain the cause of these high concentrations of salts, which appear to be due to factors beyond SWI. Additionally, the WQI results suggest

that the thresholds stipulated in water quality standards are sometimes high enough to pass groundwater with reasonably high ion contents as good drinking water as observed in W1–W4, W7–W10, and W14 (Table 9). This observation is comparable with studies on other aquifers. For instance, a study on the Hajeb Layoun-Jelma basin in central Tunisia identifies the groundwater of the shallow aquifer as Na-Cl and Ca–Mg–Cl type but the water is largely suitable for drinking according to the WHO standards except in a few cases with high salinity levels (Aouiti et al. 2021).

Integrated characterization of the groundwater

Prior related studies generally interpreted the results of different groundwater characterization approaches separately and did not link the results of the multiple approaches together (Kura et al. 2014; Idowu et al. 2017; Alfaifi et al. 2019). By combining the GALDIT overlay index, with the GQI_{SWI} , the Stuyfzand TH classification scheme, and WQI some holistic observations on the groundwater characteristics could be made. The surface maps created for each classification scheme using spatial interpolation tools also helped elucidate more on the geochemistry. The results of the GALDIT overlay index which classifies the vulnerability of the aquifer into low (29%), moderate (59%), and high (12%) vulnerabilities (Table 7), are comparable with that of the GQI_{SWI} that categorizes the aquifer into 68% and 32% brackish and saline water, respectively (Fig. 5). Vulnerability to seawater intrusion is not necessarily the same as the seawater intrusion status of a coastal aquifer. Hence, the vulnerability percentages of the GQI_{SWI} variations do not exactly

match in both figures (Figs. 4 and 5). However, it can be inferred that areas under moderate or high vulnerabilities according to GALDIT tend to have Na-Cl water type as shown in Table 9 where the GQI_{SWI} classifies all the samples as mixed groundwater of Na-Cl water type.

Throwing Stuyfzand's TH-based classification into the discussion, the TH values range from a minimum value of 0.36 to a maximum value of 2.60 and an average of 1.25 (Table 9). These values indicate that the natural occurrence of the groundwater is the [F Fb B Bs], which stands for "Fresh," "Fresh-brackish," "Brackish," and "Brackish-salt," respectively (Table 3). This classification agrees with the earlier GQI_{SWI} classification that identifies the groundwater as brackish or saline (Table 9). It can also be observed that the same water type (Na-Cl water type based on GQI_{SWI}) may produce a wide range of water hardness from soft to hard. Although Stuyfzand's TH-based classification gives a relatively broader description of the groundwater than the GQI_{SWI} classification system, it can act as a preliminary check into the nature of the groundwater. In other words, GQI_{SWI} classification can narrow down the observations from Stuyfzand's TH-based classification system.

The first observation when the WQI classification is considered alongside the other approaches is that WQI values for the WHO and national standards can vary. For instance, the mean WQI value obtained for the WHO is 106 which indicates that the groundwater largely falls under the poor water category while the WQI value of 85 observed for the national standard is indicative of good water quality in this study. A more overarching observation is that WQI values of the groundwater have no direct association with the softness or hardness of the water. For instance, "very soft" water can be a "very poor" quality drinking water (Table 9 line 5) and "hard" water can be "good" drinking water. Also, the fact that the WQI maps do not have similar trends to the GALDIT vulnerability and GQI_{SWI} maps (Figs. 4, 5, and 7) suggests that water quality in coastal aquifers is not solely determined by seawater intrusion.

Policy implications

In redefining the roles of the government towards achieving the sustainable management of groundwater in sub-Saharan Africa, the following points have been highlighted:

1. Aquifer-level resource planning
2. Stakeholder engagement and participation
3. Administration of groundwater use
4. Ground waste and wastewater discharge control
5. Groundwater monitoring and information provision and,
6. Land surface zoning for groundwater conservation" (Tuinhof et al. 2011)

By linking the above roles with the findings of this study, the first observation is that the vulnerability map (Fig. 4) and other groundwater characterization maps (Figs. 5, 6, and 7) can be valuable for the land surface zoning for groundwater conservation in the study area (no. 6). The maps can be a basis for locating special control areas such as portions extremely prone to SWI where groundwater abstraction is prohibited to avoid further deterioration. Furthermore, the methodology for creating a geodata-base outlined in this study (Fig. 1) can act as a guide for creating a continuous and temporal groundwater monitoring regime for the study area and similar coastal aquifers (no. 5).

In summary, the methodology presented in this study where GALDIT overlay index and geospatial and analytical approaches were combined can act as a valuable template for the management and continuous monitoring of coastal aquifers. The results of this study contribute further insights into the status of groundwater in the coastal regions of Kenya and the impacts of SWI in the region. Additionally, the study demonstrates the importance and relevance of geospatial techniques in developing the knowledge base required for sustainable groundwater management decision-making. The findings of the study will inform policymakers and the relevant water resource management towards developing new solutions or improving existing solutions for managing groundwater and increasing access to potable water. By extension, the solutions can further contribute to the achievement of Goal 6 of the Sustainable Development Goals which aims to ensure clean water and sanitation for all.

Conclusion

In this study, the coastal aquifer of Mombasa North Coast was extensively studied using a combination of different approaches that complement each other for creating a detailed understanding of the aquifer. The approaches used include the GALDIT overlay index, seawater intrusion groundwater quality index GQI_{SWI} , total hardness computation based on Stuyfzand's classification system, and the Water Quality Index (WQI) based on the WHO guidelines and the created a more visual understanding of the groundwater condition in the study area. The considerable standard deviation values of the groundwater hydrochemical parameters indicate a wide variation across the aquifer. The study suggests that areas under moderate or high vulnerabilities to seawater intrusion tend to have Na-Cl water type. It is also possible for a similar water type (Na-Cl water type based on GQI_{SWI}) to produce a wide range of water hardness from soft to hard. GQI_{SWI} classification can narrow down the observations from Stuyfzand's TH-based classification system. Additionally, WQI values of the groundwater have no direct association with the softness or hardness of the water. Findings from the GALDIT

index suggest that the coastal aquifer is largely experiencing a moderate impact of SWI intrusion (59%). The GQI_{SWI} assessment shows that 68% of the aquifer's coverage is characterized by brackish water while the water type is of the NaCl type impacted by salinity (domain II). The GALDIT and GQI_{SWI} add credence to previous groundwater studies in the study area. Although the values indicate the presence of SWI in moderate levels, the total hardness and WQI analyses results do not suggest that the groundwater poses any major health risks based on its chemical compositions. However, it is recommended that further studies on temporal scales be done. The findings of this study provide a baseline for subsequent studies on the coastal aquifer of Mombasa North coast and the methodology introduced can act as a template for similar studies in other regions.

Supplementary Information The online version contains supplementary material available at <https://doi.org/10.1007/s11356-021-18084-z>.

Acknowledgements The authors wish to acknowledge the African Union Commission and her partners, through the Pan African University (PAUSTI) scholarship for providing the funds for conducting the research, JICA for providing seed funds at the preliminary stage of the research, Jomo Kenyatta University of Agriculture and Technology for making facilities available as the host university for PAUSTI, and the Technical University of Kenya for technical support and access to academic materials online.

Author contribution TI was involved in the conceptualization, methodology, field data collection, laboratory tests, data analysis and investigation, and writing. MN supervised the study from the conceptualization to the manuscript writing and was involved at every stage. MK co-supervised the project and was involved from the conceptualization to the manuscript writing stage. CJ worked on parts of the methodology, especially the GIS analysis part, and also contributed to the writing of the manuscript. RW contributed to the data analysis and the GALDIT index. JM, KL, NK, and FA all contributed to original draft preparation, review, and editing. All authors read and approved the final manuscript.

Funding Funding for the project is from the African Union and her partners through the Pan African University scholarship. The funding covers all aspects of the research including data collection, analysis, and interpretation of data.

Availability of data and materials The datasets generated and/or analysed during the current study are available in the Figshare repository, <https://doi.org/10.6084/m9.figshare.9730157.v1>

Declarations

Ethics approval and consent to participate Not applicable.

Consent for publication Not applicable.

Competing interests The authors declare no competing interests.

References

- Abuodha PA (2004) Geomorphology of the Kenyan coast: Not as a result of sea level change alone. *Mozambique*
- Ajibade FO, Olajire OO, Ajibade TF et al (2021) Groundwater potential assessment as a preliminary step to solving water scarcity challenges in Ekpoma, Edo State, Nigeria. *Acta Geophys.* <https://doi.org/10.1007/s11600-021-00611-8>
- Akoteyon IS, Balogun II, Soneye ASO (2018) Integrated approaches to groundwater quality assessment and hydrochemical processes in Lagos, Nigeria. *Appl Water Sci* 8:1–19. <https://doi.org/10.1007/s13201-018-0847-y>
- Al-Abadi AM (2017) The application of Dempster-Shafer theory of evidence for assessing groundwater vulnerability at Galal Badra basin, Wasit governorate, east of Iraq. *Appl Water Sci* 7:1725–1740. <https://doi.org/10.1007/s13201-015-0342-7>
- Aladejana JA, Kalin RM, Sentenac P, Hassan I (2020) Assessing the impact of climate change on groundwater quality of the shallow coastal aquifer of Eastern Dahomey Basin, Southwestern Nigeria. *Water* 12:1–19. <https://doi.org/10.3390/w12010224>
- Alastal KM, Alagha JS, Abuhabib AA, Ababou R (2015) Groundwater quality assessment using Water Quality Index (WQI) Approach: Gaza Coastal Aquifer case study. *J Eng Res Technol* 2:80–86
- Alfaifi H, Kahal A, Albassam A et al (2019) Integrated geophysical and hydrochemical investigations for seawater intrusion : a case study in southwestern Saudi Arabia. *Arab J Geosci* 12.<https://doi.org/10.1007/s12517-019-4540-8>
- Alfarrah N, Walraevens K (2018) Groundwater overexploitation and seawater intrusion in coastal areas of arid and semi-arid regions. *Water (Switzerland)* 10.<https://doi.org/10.3390/w10020143>
- Aller L, Bennett T, Lehr J et al (1987) DRASTIC: a standardized system for evaluation ground water pollution potential using hydro-geological settings
- Amarni N, Fernane L, Naili M et al (2020) Mapping of the vulnerability to marine intrusion “in coastal Cherchell aquifer, Central Algeria” using the GALDIT method. *Groundw Sustain Dev* 11:100481. <https://doi.org/10.1016/j.gsd.2020.100481>
- Aminiyan MM, Aminiyan FM (2020) Comprehensive integrated index-based geochemistry and hydrochemical analyses of groundwater resources for multiple consumptions under coastal conditions. *Environ Sci Pollut Res* 27:21386–21406. <https://doi.org/10.1007/s11356-020-08300-7>
- Aouiti S, Hamzaoui Azaza F, El Melki F et al (2021) Groundwater quality assessment for different uses using various water quality indices in semi-arid region of central Tunisia. *Environ Sci Pollut Res* 28:46669–46691. <https://doi.org/10.1007/s11356-020-11149-5>
- Appelo CAJ, Postma D (2005) *Geochemistry, Groundwater and Pollution*, 2nd edn. CRC Press, London
- ASCE (2012) Appendix A- Conversion Tables. In: Wallender WW, Tanji KK (eds) *Agricultural Salinity Assessment and Management*, 2nd edn. pp 1071–1075
- Ayed B, Jmal I, Sahal S, Bouri S (2018) The seawater intrusion assessment in coastal aquifers using GALDIT method and groundwater quality index: the Djefara of Medenine coastal aquifer (Southeastern Tunisia). *Arab J Geosci* 11.<https://doi.org/10.1007/s12517-018-3966-8>
- Barlow PM (2003) *Ground water in freshwater-saltwater environments of the Atlantic Coast*. VA: U.S.A
- Barzegar R, Razzagh S, Quilty J et al (2021) Improving GALDIT-based groundwater vulnerability predictive mapping using coupled resampling algorithms and machine learning models. *J Hydrol* 598:126370. <https://doi.org/10.1016/j.jhydrol.2021.126370>

- Bear J, Cheng AHD, Sorek S et al (1999) Seawater intrusion in coastal aquifers: concepts, methods and practices, (Vol. 14). Springer Science & Business Media
- Bordbar M, Neshat A, Javadi S (2019) Modification of the GALDIT framework using statistical and entropy models to assess coastal aquifer vulnerability. *Hydrol Sci J* 64:1117–1128. <https://doi.org/10.1080/02626667.2019.1620951>
- Bordbar M, Neshat A, Javadi S et al (2021) Improving the coastal aquifers' vulnerability assessment using SCMAI ensemble of three machine learning approaches. *Nat Hazards*. <https://doi.org/10.1007/s11069-021-05013-z>
- Bouderbala A (2017) Assessment of Water Quality Index for the groundwater in the upper Chelif Plain, Algeria. *J Geol Soc India* 90:347–356. <https://doi.org/10.1007/s12594-017-0723-7>
- Bouderbala A, Remini B, Hamoudi AS, Pulido-Bosch A (2016) Assessment of groundwater vulnerability and quality in coastal aquifers : a case study (Tipaza , North Algeria). *Arab J Geosci* 9.<https://doi.org/10.1007/s12517-015-2151-6>
- Caswell V (1954a) Geology of the Kilifi-Mazeras area degree sheet 66 SE quarter [Map]. Map
- Caswell V (1954b) Geology of the Mombasa-Kwale area degree sheet 69 ; with coloured map [Map]. Map
- Caswell V (2007) Geology of the kilifi-mazeras area (Report No 34, pp. 1–54). Nairobi.
- Chachadi A, Lobo-Ferreira J (2001b) Seawater Intrusion Vulnerability Mapping of Aquifers Using GALDIT Method. TERI, COASTIN a Coast Policy Res Newsl
- Chachadi AG, Lobo-Ferreira JP (2005) Assessing aquifer vulnerability to sea-water intrusion using GALDIT method: Part 2— GALDIT indicators description. In: Fourth Inter-Celtic Colloquium on Hydrogeology and Management of Water Resources. IAHS Publ, Portugal
- Chachadi A, Lobo-Ferreira J (2001a) Sea water intrusion vulnerability mapping of aquifers using GALDIT method. *Coastin* 4:7–9
- Chang SW, Chung I-M, Kim M-G et al (2019) Application of GALDIT in assessing the seawater intrusion vulnerability of Jeju Island. *South Korea Water* 11:1824. <https://doi.org/10.3390/w11091824>
- Chaurasia AK, Pandey HK, Tiwari SK et al (2018) Groundwater quality assessment using Water Quality Index (WQI) in parts of Varanasi District, Uttar Pradesh, India. *J Geol Soc India* 92:76–82. <https://doi.org/10.1007/s12594-018-0955-1>
- Childs C (2009) The Top Nine Reasons to Use a File Geodatabase. 12–15
- Civita M, Regibus DC (1995) Sperimentazione di alcune metodologie per la valutazione della vulnerabilità degli acquiferi. *Q Geol Appl Pitagora*, Bol 3:
- Civita M (1994) La carte della vulnerabilità 'deli aquifer all' inquinamento: teoria & pratica (Aquifer vulnerability maps to pollution). Pitagora Ed Bol
- Climatemp (2017) Mombasa Climate & Temperature. <http://www.mombasa.climatemp.com/>. Accessed 9 Nov 2019
- Kenya Coast (2011) Kenya Coast Weather. In: Kenya Coast. <http://kenya-coast.com/en/item/kenya-coast-weather>. Accessed 9 Nov 2019
- CPH (2021) Kriging Interpolation. In: Columbia Public Heal. <https://www.publichealth.columbia.edu/research/population-health-methods/kriging-interpolation>. Accessed 10 Oct 2021
- Darnault CJ, Godinez I (2008) Coastal Aquifers and Seawater intrusion. In: Darnault CJ (ed) Overexploitation and contamination of shared groundwater resources. Springer science+Business Media B. V., New York, pp 185–201
- Doerfliger N, Zwahlen F (1997) EPIK: a new method for outlining of protection areas in karstic environment. In: Gü- nay G, Jonshon A (eds) International symposium and field seminar on “karst waters and environmental impacts. Antalya, Turkey. Balkema, Rotterdam, pp 117–123
- Eguaroje EO, A AT, O OJ et al (2015) Flood vulnerability assessment of Ibadan City, Oyo State, Nigeria. *World Environ* 5:149–159. <https://doi.org/10.5923/j.env.20150504.03>
- El Bilali A, Taleb A, Nafii A et al (2021) Prediction of sodium adsorption ratio and chloride concentration in a coastal aquifer under seawater intrusion using machine learning models. *Environ Technol Innov* 23:101641. <https://doi.org/10.1016/j.eti.2021.101641>
- ESRI (2019) How inverse distance weighted interpolation works. <https://pro.arcgis.com/en/pro-app/help/analysis/geostatistical-analyst/how-inverse-distance-weighted-interpolation-works.htm>. Accessed 28 Oct 2019
- Etsias G, Hamill GA, Benner EM et al (2020) Optimizing Laboratory Investigations of Saline Intrusion by Incorporating Machine Learning Techniques. *Water* 12
- Ezekiel IT, Maurice N, Maurice K (2016) Seawater intrusion vulnerability assessment of a coastal aquifer : north coast of Mombasa, Kenya as a case study. *Int J Eng Res Appl* 6(8):37–45
- Foster S (1987) Fundamental concepts in aquifer vulnerability, pollution risk and protection strategy. In: Van Duijvendooden W, van Waegeningh H (eds) Vulnerability of soil and groundwater to pollutions: proceedings and information. TNO Committee on Hydrological Research, The Hague, pp 69–86
- Goodchild MF, Haining RP (2003) GIS and Spatial Data Analysis : Converging Perspectives. *Pap Reg Sci* 83:363–385. <https://doi.org/10.1007/s10110-003-0190-y>
- Hajji S, Nasri G, Boughariou E et al (2020) Towards understanding groundwater quality using hydrochemical and statistical approaches: case of shallow aquifer of Mahdia-Ksour Essaf (Sahel of Tunisia). *Environ Sci Pollut Res* 27:5251–5265. <https://doi.org/10.1007/s11356-019-06982-2>
- Hamlat A, Guidoum A (2018) Assessment of groundwater quality in a semi-arid region of Northwestern Algeria using water quality index (WQI). *Appl Water Sci* 8:1–13. <https://doi.org/10.1007/s13201-018-0863-y>
- Herbert ER, Schubauer-Berigan J, Craft CB (2018) Differential effects of chronic and acute simulated seawater intrusion on tidal freshwater marsh carbon cycling. *Biogeochemistry* 138:137–154. <https://doi.org/10.1007/s10533-018-0436-z>
- Heydarirad L, Mosaferi M, Pourakbar M et al (2019) Groundwater salinity and quality assessment using multivariate statistical and hydrogeochemical analysis along the Urmia Lake coastal in Azarshahr plain, North West of Iran. *Environ Earth Sci* 78:1–16. <https://doi.org/10.1007/s12665-019-8655-8>
- Hsu S-Y (2005) Effects of flow rate, temperature and salt concentration on chemical and physical properties of electrolyzed oxidizing water. *J Food Eng* 66:171–176. <https://doi.org/10.1016/j.jfoodeng.2004.03.003>
- Idowu TE (2017) Groundwater flow and quality of coastal aquifers : case study of Mombasa North Coast. Jomo Kenyatta University of Agriculture and Technology, Kenya
- Idowu TE, Lasisi KH (2020) Seawater intrusion in the coastal aquifers of East and Horn of Africa: a review from a regional perspective. *Sci African* 8:1–15. <https://doi.org/10.1016/j.sciaf.2020.e00402>
- Idowu TE, Nyadawa M, K'Orowe MO (2017) Hydrogeochemical assessment of a coastal aquifer using statistical and geospatial techniques: case study of Mombasa North Coast. *Kenya Environ Earth Sci* 76:422. <https://doi.org/10.1007/s12665-017-6738-y>
- Idowu TE, Waswa RM, Lasisi K et al (2020) Towards achieving sustainability of coastal environments : urban growth analysis and prediction of Lagos State, Nigeria. *South African J Geomatics* 9:149–162. <https://doi.org/10.4314/sajg.v9i2.11>
- Idowu TE, Home PG (2015) Probable effects of sea level rise and land reclamation activities on coastlines and wetlands. In: The 2015 JKUAT Scientific Conference. JKUAT, Nairobi, pp 207–220

- Iidowu TE, Nyadawa M, K'orowe M (2018) Assessment of groundwater salinity and impact of seawater intrusion on a coastal aquifer: north coast of Mombasa as case study. In: *Advancing Africa's Sustainable Development: Proceedings of the 4th Conference on Science Advancement*. Cambridge Scholars Publishing, Nairobi, p 295
- Igrac (2017) Transboundary aquifers of the world map. In: *Int. Groundw. Resour. Assess. Cent.* <https://apps.geodan.nl/igrac/ggis-viewer/viewer/transboundary/public/default>. Accessed 7 Jun 2019
- Karami S, Madani H, Katibeh H, Fatehi Marj A (2018) Assessment and modeling of the groundwater hydrogeochemical quality parameters via geostatistical approaches. *Appl Water Sci* 8:1–13. <https://doi.org/10.1007/s13201-018-0641-x>
- KEBS (2015) KENYA STANDARDS Potable water — specification. Nairobi, Kenya
- Ketabchi H, Mahmoodzadeh D, Ataie-Ashtiani B, Simmons CT (2016) Sea-level rise impacts on seawater intrusion in coastal aquifers: review and integration. *J Hydrol* 535. <https://doi.org/10.1016/j.jhydrol.2016.01.083>
- Ketata-Rokbani M, Gueddari M, Bouhlila R (2011) Use of geographical information system and water quality index to assess Groundwater Quality in El Khairat Deep Aquifer (Enfidha, Tunisian Sahel). *Iran J Energy Environ* 2:133–144
- Kithiia J, Majambo G (2020) Motion but no speed: colonial to post-colonial status of water and sanitation service provision in Mombasa city. *Cities* 107:102867. <https://doi.org/10.1016/j.cities.2020.102867>
- Klassen J, Allen DM, Kirste D (2014) Chemical Indicators of Saltwater Intrusion for the Gulf Islands, British Columbia. *British Columbia*
- KNBS (2010) 2009 Kenya population and housing census, population distribution by political units. Nairobi, Kenya
- KNBS (2019) 2019 Kenya population and housing census Volume I: population by county and sub-county. Nairobi, Kenya
- Kogo BK, Kumar L, Koech R (2019) Forest cover dynamics and underlying driving forces affecting ecosystem services in western Kenya. *Remote Sens Appl Soc Environ* 14:75–83. <https://doi.org/10.1016/j.rsase.2019.02.007>
- Krishna-kumar S, Logeshkumaran A, Magesh NS et al (2015) Hydrogeochemistry and application of water quality index (WQI) for groundwater quality assessment, Anna Nagar, part of Chennai City, Tamil Nadu, India. *Appl Water Sci* 5:335–343. <https://doi.org/10.1007/s13201-014-0196-4>
- Kumar P, Dasgupta R, Johnson BA et al (2019) Effect of land use changes on water quality in an ephemeral coastal plain: Khambhat City, Gujarat, India. *Water (Switzerland)* 11. <https://doi.org/10.3390/w11040724>
- Kura N, Ramli M, Ibrahim S et al (2014) An integrated assessment of seawater intrusion in a small island using geophysical, geochemical and geostatistical techniques. *Env Sci Pollut Res* 21:7047–7064. <https://doi.org/10.1007/s11356-014-2598-0>
- Kura NU, Ramli MF, Ibrahim S et al (2015) Assessment of groundwater vulnerability to anthropogenic pollution and seawater intrusion in a small tropical island using index-based methods. *Environ Sci Pollut Res* 22:1512–1533. <https://doi.org/10.1007/s11356-014-3444-0>
- Lee E, Lim JW, Moon HS, Lee KK (2015) Assessment of seawater intrusion into underground oil storage cavern and prediction of its sustainability. *Environ Earth Sci* 73:1179–1190. <https://doi.org/10.1007/s12665-014-3473-5>
- Lobo-Ferreira JP, Chachadi AG, Diamantino C, Henriques MJ (2005) Assessing aquifer vulnerability to seawater intrusion using GALDIT method: Part I. In: *Publ. I (ed) Application to the Portuguese Aquifer of Monte Gordo*. Fourth Inter-Celtic Colloquium on Hydrogeology and Management of Water Resources. Portugal, pp 11–14
- Luoma S, Okkonen J, Korkka-Niemi K (2017) Comparaison des méthodes AVI, SINTACS modifiée et GALDIT d'évaluation de la vulnérabilité d'un aquifère côtier peu profond dans le Sud de la Finlande pour des scénarios de changement climatique. *Hydrogeol J* 25:203–222. <https://doi.org/10.1007/s10040-016-1471-2>
- Mahammad S, Islam A (2021) Evaluating the groundwater quality of Damodar Fan Delta (India) using fuzzy-AHP MCDM technique. *Appl Water Sci* 11:1–17. <https://doi.org/10.1007/s13201-021-01408-2>
- Mitas L, Mitasova H (1999) Spatial interpolation. In: Longley P, Goodchild MF, Maguire DJ, Rhind DW (eds) *Geographical Information Systems: Principles, Techniques, Management and Applications*, 1st edn. Wiley, pp 481–492
- Mtoni YE (2013) Saltwater intrusion in the coastal strip of Dar es Salaam Quaternary aquifer. Ghent University, Tanzania
- Munga D, Mwangi S, Ong'anda H et al (2006) Vulnerability and pollution of groundwater in Kisauni, Mombasa, Kenya. *Groundw Pollut Africa Taylor Fr* 213–228
- Mwamburi EK (2013) Factors affecting access of supply in Kisauni area, Mombasa county. University of Nairobi, Kenya
- Naseem S, Bashir E, Ahmed P et al (2018) Impact of seawater intrusion on the geochemistry of groundwater of Gwadar district, Balochistan and its appraisal for drinking water quality. *Arab J Sci Eng* 43:281–293. <https://doi.org/10.1007/s13369-017-2679-8>
- Nlend B, Celle-Jeanton H, Huneau F et al (2018) The impact of urban development on aquifers in large coastal cities of West Africa: present status and future challenges. *Land Use Policy* 75:352–363. <https://doi.org/10.1016/j.landusepol.2018.03.007>
- Okello C, Tomasello B, Greggio N et al (2015) Impact of population growth and climate change on the freshwater resources of Lamu Island, Kenya. *Water* 7:1264–1290. <https://doi.org/10.3390/w7031264>
- Rizwan R, Gurdeep S (2010) Assessment of ground water quality status by using water quality index method in Orissa, India. *World Appl Sci J* 9:1392–1397
- Sahu P, Sikdar PK (2008) Hydrochemical framework of the aquifer in and around East Kolkata Wetlands, West Bengal, India. *Environ Geol* 55:823–835. <https://doi.org/10.1007/s00254-007-1034-x>
- Sarath Prasanth SV, Magesh NS, Jitheshlal KV et al (2012) Evaluation of groundwater quality and its suitability for drinking and agricultural use in the coastal stretch of Alappuzha District, Kerala, India. *Appl Water Sci* 2:165–175. <https://doi.org/10.1007/s13201-012-0042-5>
- Sarkar B, Islam A, Majumder A (2021) Seawater intrusion into groundwater and its impact on irrigation and agriculture: Evidence from the coastal region of West Bengal. *India Reg Stud Mar Sci* 44:101751. <https://doi.org/10.1016/j.rsma.2021.101751>
- Seenipandi K, Nainarpandian C, Kandathil RK, Sellamuthu S (2019) Seawater intrusion vulnerability in the coastal aquifers of southern India—an appraisal of the GALDIT model, parameters' sensitivity, and hydrochemical indicators. *Environ Sci Pollut Res* 26:9755–9784. <https://doi.org/10.1007/s11356-019-04401-0>
- Shammi M, Rahman MM, Bondad SE, Bodrud-Doza M (2019) Impacts of salinity intrusion in community health: A review of experiences on drinking water sodium from coastal areas of Bangladesh. *Healthc* 7. <https://doi.org/10.3390/healthcare7010050>
- Siyal AA (2018) Climate Change : Assessing Impact of Seawater Intrusion on Soil , Water and Environment on Indus Delta Using GIS and Remote Sensing Tools. Jamshoro, Pakistan
- Sophiya SM, Syed TH (2013) Assessment of vulnerability to seawater intrusion and potential remediation measures for coastal aquifers: a case study from eastern India. *Environ Earth Sci* 70:1197–1209. <https://doi.org/10.1007/s12665-012-2206-x>

- Stein S, Sola F, Yechieli Y et al (2020) The effects of long-term saline groundwater pumping for desalination on the fresh–saline water interface: field observations and numerical modeling. *Sci Total Environ* 732:139249. <https://doi.org/10.1016/j.scitotenv.2020.139249>
- Stuyfzand P (1986) A new hydrochemical classification of watertypes: principles and application to the coastal dunes aquifer system of the Netherlands. *Proc Ninth Salt Water Intrusion Meet* 641–655
- Stuyfzand PJ (1993) Hydrochemistry and hydrology of the coastal dune area of the Western Netherlands. Vrije Universiteit Amsterdam
- Sudaryanto, Nailly W (2018) Ratio of major ions in groundwater to determine saltwater intrusion in coastal areas. *IOP Conf Ser Earth Environ Sci* 118. <https://doi.org/10.1088/1755-1315/118/1/012021>
- Sundaram VLK, Dinesh G, Ravikumar G, Govindarajulu D (2008) Vulnerability assessment of seawater intrusion and effect of artificial recharge in Pondicherry coastal region using GIS. *Indian J Sci Technol* 1:1–7. <https://doi.org/10.17485/ijst/2008/v1i7/29593>
- Tomaszkiewicz M, Abou Najm M, El-Fadel M (2014) Development of a groundwater quality index for seawater intrusion in coastal aquifers. *Environ Model Softw* 57:13–26. <https://doi.org/10.1016/j.envsoft.2014.03.010>
- Trabelsi N, Triki I, Hentati I, Zairi M (2016) Aquifer vulnerability and seawater intrusion risk using GALDIT, QGISWI and GIS: case of a coastal aquifer in Tunisia'. *Environ Earth Sci* 75
- Tuinhof A, Foster S, Frank van Steenbergen, Talbi A, Wishart M (2011) Appropriate groundwater management policy for Sub-Saharan Africa in face of demographic pressure and climatic variability
- Vaiphei SP, Kurakalva RM, Sahadevan DK (2020) Water quality index and GIS-based technique for assessment of groundwater quality in Wanaparthy watershed, Telangana, India. *Environ Sci Pollut Res* 27:45041–45062. <https://doi.org/10.1007/s11356-020-10345-7>
- Van Stempvoort D, Evert L, Wassenaar L (1993) Aquifer vulnerability index: a GIS compatible method for groundwater vulnerability mapping. *Can Wat Res J* 18:25–37
- Vengadesan M, Lakshmanan E (2019) Management of Coastal Groundwater Resources. In: Krishnamurthy RR, Jonathan MP, Srinivasalu S, Glaeser B (eds) *COASTAL MANAGEMENT: Global Challenges and Innovations*. Academic Press, Elsevier, pp 383–397
- Verruijt A (1968) A note on GHyben-Herzberg Formula. *Bull Int Assoc Sci Hydrol* XIII:4–12
- Vu DT, Yamada T, Ishidaira H (2018) Assessing the impact of sea level rise due to climate change on seawater intrusion in Mekong Delta. *Vietnam Water Sci Technol* 77:1632–1639. <https://doi.org/10.2166/wst.2018.038>
- Wei A, Li D, Dai F et al (2021) An optimization method coupled the index-overlay method with entropy weighting model to assess seawater intrusion vulnerability. *Environ Sci Pollut Res*. <https://doi.org/10.1007/s11356-021-13229-6>
- Werner AD, Bakker M, Post VEA et al (2013) Seawater intrusion processes, investigation and management: Recent advances and future challenges. *Adv Water Resour* 51:3–26. <https://doi.org/10.1016/j.advwatres.2012.03.004>
- WHO (2011) *Hardness in Drinking-water: Background document for development of WHO Guidelines for Drinking-water Quality*. Geneva, Switzerland
- WHO (2017) *Guidelines for drinking-water quality: fourth edition incorporating the first addendum*. Geneva Switzerland
- Witkowski AJ, Kowalczyk A, Vrba J (2014) *Groundwater vulnerability assessment and mapping: IAH-selected papers, vol 11*. CRC Press
- Wong PP, Losada JJ, Gattuso J-P et al (2014) Coastal systems and low-lying areas. In: *Climate change 2014: impacts, adaptation, and vulnerability. Part A: Global and Sectoral Aspects*. New York, NY, USA, pp 361–409

Publisher's note Springer Nature remains neutral with regard to jurisdictional claims in published maps and institutional affiliations.